Title

A comparison of numerical and machine-learning modeling of soil water content with limited input data

Authors

Karandish, Fatemeh
Šimůnek, Jiří

Publication Date

2016-12-01

DOI

10.1016/j.jhydrol.2016.11.007

Peer reviewed

Journal of Hydrology 543 (2016) 892–909

Contents lists available at ScienceDirect

Journal of Hydrology

journal homepage: www.elsevier.com/locate/jhydrol

Research papers

A comparison of numerical and machine-learning modeling of soil water content with limited input data

Fatemeh Karandish [a,*], Jiří Šimůnek [b]

[a] Water Engineering Department, University of Zabol, Zabol, Iran
[b] Department of Environmental Sciences, University of California Riverside, Riverside, CA 92521, USA

ARTICLE INFO

Article history:
Received 22 October 2016
Received in revised form 3 November 2016
Accepted 5 November 2016
Available online 8 November 2016
This manuscript was handled by P. Kitanidis, Editor-in-Chief, with the assistance of Juan V. Giraldez, Associate Editor

Keywords:
Machine-learning models
ANFIS
HYDRUS-2D
MLR
SVM
Soil water content
Water saving irrigation

ABSTRACT

Soil water content (SWC) is a key factor in optimizing the usage of water resources in agriculture since it provides information to make an accurate estimation of crop water demand. Methods for predicting SWC that have simple data requirements are needed to achieve an optimal irrigation schedule, especially for various water-saving irrigation strategies that are required to resolve both food and water security issues under conditions of water shortages. Thus, a two-year field investigation was carried out to provide a dataset to compare the effectiveness of HYDRUS-2D, a physically-based numerical model, with various machine-learning models, including Multiple Linear Regressions (MLR), Adaptive Neuro-Fuzzy Inference Systems (ANFIS), and Support Vector Machines (SVM), for simulating time series of SWC data under water stress conditions. SWC was monitored using TDRs during the maize growing seasons of 2010 and 2011. Eight combinations of six, simple, independent parameters, including pan evaporation and average air temperature as atmospheric parameters, cumulative growth degree days (*cGDD*) and crop coefficient (K_c) as crop factors, and water deficit (*WD*) and irrigation depth (*In*) as crop stress factors, were adopted for the estimation of SWCs in the machine-learning models. Having Root Mean Square Errors (RMSE) in the range of 0.54–2.07 mm, HYDRUS-2D ranked first for the SWC estimation, while the ANFIS and SVM models with input datasets of *cGDD*, K_c, *WD* and *In* ranked next with RMSEs ranging from 1.27 to 1.9 mm and mean bias errors of −0.07 to 0.27 mm, respectively. However, the MLR models did not perform well for SWC forecasting, mainly due to non-linear changes of SWCs under the irrigation process. The results demonstrated that despite requiring only simple input data, the ANFIS and SVM models could be favorably used for SWC predictions under water stress conditions, especially when there is a lack of data. However, process-based numerical models are undoubtedly a better choice for predicting SWCs with lower uncertainties when required data are available, and thus for designing water saving strategies for agriculture and for other environmental applications requiring estimates of SWCs.

1. Introduction

Because it uses about 70% of the world's freshwater withdrawals (OECD, 2010), agriculture is a primary target for policies that move the sector towards sustainable management of water. Over past decades, irrigated agriculture has been widely developed around the world as it significantly increases crop productivity. However, irrigation consumes high volumes of water and may induce off-site pollution of receiving water bodies (Billib et al., 2009). Thus, special attention should be paid to the water management of irrigated lands. Water should be applied in the right amount at the right time in order to achieve an optimal crop production and it should not be wasted as it is a valuable resource, and its applications should be environmentally sustainable (SAI, 2010).

An optimal irrigation schedule created by accurately estimating the crop water demand (CWD) may help achieve these goals since it prevents both yield and water losses (Payero et al., 2006; Klocke et al., 2004; Stone, 2003). Among different developed methods, estimating CWD based on the soil water balance is commonly advised (Allen et al., 2011) since it considers real CWD, which may produce significant water savings in irrigated agriculture. Applying this method for irrigation scheduling requires knowledge about temporal variations of soil water contents (SWCs) at the field scale for crops both under optimal or water-stress conditions in a soil-plant continuum. This is because the plant water status, which is a dominant factor determining the crop yield (Taiz and Zeiger,

* Corresponding author.
E-mail addresses: F.Karandish@uoz.ac.ir, Karandish_h@yahoo.com (F. Karandish).

http://dx.doi.org/10.1016/j.jhydrol.2016.11.007
0022-1694/

2006), is closely related to SWC (Dorji et al., 2005; Simon et al., 2009; Souza et al., 2009; Stoll et al., 2000; Xu, 2009). Thus, in order to achieve the highest irrigation water use efficiency, the reduction of irrigation should be done only to the extent that SWC is kept under optimal conditions to avoid a significant reduction in yield.

The need for suitable methods of estimating SWCs under water stress conditions becomes more obvious when it is understood that the scarcity of fresh water is an increasingly global problem (Karandish et al., 2015), resulting from a gradual increase in food demand and a decrease in available fresh water resources, that needs to be urgently resolved (Sepaskhah and Ahmadi, 2010). Under these circumstances, it is necessary to adopt water saving irrigation strategies to cope with actual water availability. Partial root zone drying (PRD) is a new deficit irrigation strategy, which may produce water savings without a significant decrease in yields (Dry et al., 2000; Kang and Zhang, 2004; Kirda et al., 2004; Shao et al., 2008; Tang et al., 2005; Karandish and Šimůnek, 2016). Under the PRD strategy, which was introduced by Dry and Loveys (1998), one half of the root zone is irrigated while the other half is dried out. Irrigated and dry sides of the root zone are periodically switched. Good knowledge of root zone SWCs greatly influences the efficiency of PRD since the time of the irrigation shift should be determined based on the soil water matric potential in order to produce optimal results.

Despite of the importance of directly determining SWCs as a time series, the inability of doing so in the field at a low cost represents a restriction on the application of the soil water balance equation for irrigation scheduling, especially in the planning and optimizing stages of irrigation projects. Thus, further attempts are required to find suitable methods for indirectly estimating SWCs. In this regard, different models have been developed for simulating SWCs in soil-crop systems during the past three decades. SWCs can be estimated using either simple soil water balance models, which require only limited input information (Wessolek, 1989; Cameira et al., 2003; Panigrahi and Panda, 2003; Nishat et al., 2007), or more complex process-based models such as LEACHM (Wagenet and Hutson, 1987), GLEAMS (Leonard et al., 1987), WAVE 2.1 (Vanclooster et al., 1996; Fernández et al., 2002), EURO-ACCESS-II (Armstrong et al., 1996; Fernández et al., 2002), SWIM (Verburg et al., 1996), SWAP (van Dam et al., 1997), SWAT (Neitsch et al., 2005), or HYDRUS (Šimůnek et al., 2008, 2016), which require a large number of input parameters. However, since these parameters are directly related to soil, crop, and climate properties, these models often provide superior predictions of SWCs than simpler soil water balance models.

HYDRUS-2D (Šimůnek et al., 2008, 2016) is one of the dynamic, physically based models that is widely used to simulate soil water dynamics (e.g., Cote et al., 2003; Skaggs et al., 2004; Ajdary et al., 2007; Rahil, 2007; Crevoisier et al., 2008; Lazarovitch et al., 2009; Siyal and Skaggs, 2009; Mubarak, 2009; Ramos et al., 2012; Tafteh and Sepaskhah, 2012). One of the advantages of this model is that its parameters are related to soil physical properties, which may be measured either in-situ or in the lab. There are many published studies in which HYDRUS-2D was applied to evaluate temporal variations of soil-water-plant interactions, including under the PRD conditions (Karandish and Šimůnek, 2016). Karandish and Šimůnek (2016) demonstrated the high capability of the model to simulate temporal variations of various soil water balance components under full irrigation, deficit irrigation, and PRD conditions. However, HYDRUS-2D requires the determination of soil hydraulic parameters and exact initial and boundary conditions, which sometimes hampers its more widespread use.

Machine-learning approaches, such as artificial neural networks (ANN) and support vector machines (SVM), are another group of models that have been applied during past decades for simulating various hydrological processes including soil water dynamics (Jiang and Cotton, 2004; Ahmad and Simonovic, 2005; Elshorbagy and Parasuraman, 2008; Zou et al., 2010; Dai et al., 2011; Asefa et al., 2006; Yu and Liong, 2007; Lin et al., 2009; Liu et al., 2010; Deng et al., 2011). These approaches provide a great prediction capacity and do not require the knowledge of soil physical properties. On the other hand, they do require meteorological measurements and time-series of various soil variables such as soil water contents or matric potentials as training data. Therefore, their prediction capability is limited by information contained in the data. Also, they do not have direct intuitive interpretation (Lamorski et al., 2013) with respect to evaluated processes. Literature reviews also revealed that another powerful artificial intelligence method, the adaptive neuro-fuzzy inference systems (ANFIS), has not yet been used for simulating SWCs.

Although machine-learning models have been previously used to simulate time series of SWC variations, the emphasis usually was on estimating future SWCs from their historic values (i.e., from soil water contents measured on previous days). However, this is a rather restrictive use of these models, since it is hard to use this approach to determine irrigation scheduling, especially during the planning stages. This problem becomes more severe when the focus is on optimization problems and finding the optimal water-saving irrigation schedule.

In addition, the earlier applications of machine-learning models were all for non-stressed conditions under full irrigation. However, it is becoming more difficult to irrigate crops to meet their full demand when water is in short supply, so models must be able to accurately predict SWCs for stressed conditions as well. Thus, the objectives of this study were to use both the machine-learning and physically-based models to predict time series of SWCs in the rooting depth of maize under full irrigation as well as under several different water saving irrigation strategies. The physically-based HYDRUS-2D model was used to simulate temporal variations of SWCs under PRD treatments. Its predictions were compared with predictions of the multiple linear regressions (MLR), ANFIS, and SVM models, which only require the knowledge of simple and easily determined atmospheric and crop parameters. Second, when only limited data is available, the possibility of substituting HYDRUS-2D with machine learning models for indirectly estimating SWCs is evaluated.

2. Materials and methods

2.1. Field investigations

The experimental site of the Sari Agricultural Sciences and Natural Resources University is located on the coastal plain of northern Iran, (36.3°N, 53.04°E, 15 m below the sea level). Mean annual rainfall is 616 mm, about 70% of which occurs during the October-March period. The long-term average, minimum, and maximum air temperatures are 17.3, −6, and 38.9 °C, respectively (Karandish and Šimůnek, 2016). Weather data were recorded daily in the experimental area. The soil physical characteristics are summarized in Table 1.

The experiment was carried in a maize field using a randomized complete block design with three surface drip irrigation treatments as described below. To measure retention curves, soil samples were taken every 20 cm to a depth of 80 cm for each treatment in three replicates before crop sowing and using a 2-in ID augur. SWCs at 11 different pressure heads were measured in the laboratory at each sample using a pressure plate apparatus. Thereafter, the van Genuchten-Mualem model (Mualem, 1976; van Genuchten, 1980) was used to describe the soil hydraulic properties. The soil hydraulic parameters for two soil horizons (i.e., 0–20 cm and 20–80 cm soil depths) were obtained by fitting this

Table 1
Soil properties at the experimental site.

Depth (cm)	Soil texture	Sand (%)	Silt (%)	Clay (%)	Field capacity (%)	Wilting point (%)	Bulk density (g cm^{-3})
0–20	Sandy clay loam	49	22	27	30	15	1.40
20–40	Clay loam	40	25	35	32	14	1.38
40–60	Clay loam	30	36	34	32	14	1.35
60–80	Clay loam	37	30	33	32	14	1.37
80–100	Clay loam	36	28	34	32	14	1.37

model to the observed retention curve data of both layers using the RETC program (van Genuchten et al., 1991). Fitted soil hydraulic parameters included the saturated SWC (θ_s), the residual SWC (θ_r), and the shape parameters α and n. Since no hydraulic conductivity data was available, the pedotransfer functions embedded in the HYDRUS-2D software were used to predict the saturated soil hydraulic conductivity (K_s) using measured soil physical properties for each treatment.

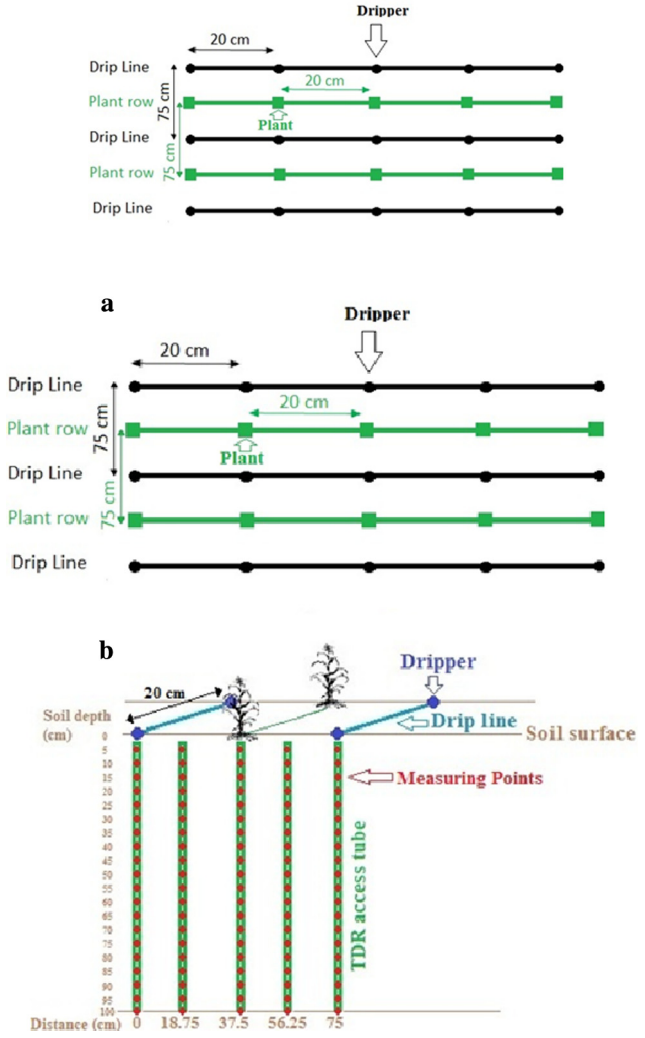

Fig. 1. Locations of drip line laterals, drippers, plants (a), and TDR probes (b) in the experimental maize field.

The surface drip irrigation system was then installed prior to crop sowing. Fig. 1a shows the locations of drip lines, drippers, and plants in the experimental field. Five Time Domain Reflectometry (TDR) access tubes (TRIME FM, IMKO, Germany) for continuous monitoring the SWCs were installed in the maize root zone of each treatment, as illustrated in Fig. 1b. TDR probes were used at least two times a day to measure soil water contents (SWCs) at depths of every 5 cm (i.e., at measuring points displayed in Fig. 1b) during both growing seasons of 2010 and 2011 (i.e., from sowing to harvest). Overall, SWCs were measured at each measuring time in 100 points for each treatment. Moreover, information about the movement of the wetting front during irrigation events was collected at least 10 times in each treatment by measuring SWCs one hour before, and immediately and 2, 6, 12, 24, 48 h after the irrigation events in the 2010 growing season. For each treatment, such SWC information was collected for at least 10 irrigation events during each growing season.

Thereafter, maize single-cross hybrid 704 was sown on May 26 of both 2010 and 2011, 5 cm deep, with 75 × 20 cm × cm crop row and crop spacing, between and parallel to the drip lines (Fig. 1a, Table 2). Crops were irrigated every other day using surface drip irrigation during the entire growing season with a total 53 and 55 irrigation events in the 2010 and 2011 growing seasons, respectively. Irrigation treatments included full irrigation (FI) and two partial root-zone drying treatments, PRD_{75} and PRD_{55}. The FI treatment was fully irrigated and the soil water content was kept close to field capacity during the entire growing season. The irrigation requirement (in mm) for the FI treatment was calculated using Eq. (1) for each irrigation event:

$$[I_n]_{FI} = \sum_{i=1}^{m} \{[\theta_{FCi} - (\theta_{BIi})_{FI}]D_i\} \quad (1)$$

where $[I_n]_{FI}$ is the net irrigation depth (mm) of the nth irrigation event for the FI treatment, θ_{FCi} is the volumetric SWC at field capacity (FC, %) of the ith soil layer, $(\theta_{BIi})_{FI}$ is the average volumetric SWC before irrigation of the ith soil layer (%) in the FI treatment, D_i is the soil layer thickness (mm), i is the soil layer, and m refers to the number of soil layers down to a specific soil depth, for which $[I_n]_{FI}$ is calculated. $(\theta_{BIi})_{FI}$ was measured using TDR probes before each irrigation event.

All treatments (including FI and both PRD treatments) received the same amount of irrigation water during the first 55 days after sowing (DAS) in 2010 and during 45 DAS in 2011. During the PRD period (i.e., during 55–107 DAS in 2010 and during 45–110 DAS in

Table 2
Summary of agricultural and fertilization activities during the maize growing season.

Date	Agricultural activities and fertilization	Remarks
May 26 in 2010 and 2011	Planting and fertilization	150 kg ha^{-1} triple superphosphate
June 12, 2010 and June 5, 2011	Fertilization	65 kg ha^{-1} urea and 50 kg ha^{-1} potassium sulphate
July 14, 2010 and July 4, 2011	Fertilization	135 kg ha^{-1} urea and 100 kg ha^{-1} potassium sulphate
July 19, 2010 and July 9, 2011	Onset PRD treatments	
September 9, 2010 and September 12, 2011	Harvest	

2011), the PRD treatments were scheduled to receive 55% (PRD_{55}) and 75% (PRD_{75}) of the FI treatment's irrigation amount at each irrigation event. While in the FI treatment, both drip lines were operated simultaneously, in the PRD treatments during the PRD period, to ensure partial root-zone drying, just one of the drip lines was operated while the other was not during each irrigation event. Only half of the root zone was thus irrigated during the PRD period, while irrigation shifted between the two sides of the plants each week. The dripper discharge was two liters per hour.

Prior to implementing the PRD treatments, the information about the movement of the wetting front was collected by measuring SWCs using TDR probes to determine the maximum lateral advance of the wetting front for different irrigation water depths. Such information was required to ensure that only about half of the rooting zone in the PRD_{75} and PRD_{55} treatments is irrigated after imposing the PRD treatments. A maximum observed lateral advance of about 35 cm confirmed this assumption.

Plants were harvested on September 9, 2010 (107 DAS) and on September 12, 2011 (110 DAS). Detailed description of all measurements during field investigation, especially those required for calibration and validation of HYDRUS-2D, is presented in Karandish and Šimůnek (2016).

2.2. HYDRUS (2D/3D)

2.2.1. Model description

HYDRUS-2D (Šimůnek et al., 2008) is a powerful software for simulating the transient, two-dimensional movement of water and nutrients in soils for a wide range of boundary conditions, and soil heterogeneities. Water flow in soils is described using the Richards equation as follows:

$$\frac{\partial \theta}{\partial t} = \frac{\partial}{\partial x}\left(K_x \frac{\partial h}{\partial x}\right) + \frac{\partial}{\partial z}\left(K_z \frac{\partial h}{\partial z}\right) - \frac{\partial k}{\partial z} - WU(h,x,z) \quad (2)$$

where θ is the volumetric SWC ($L^3\,L^{-3}$), K is the unsaturated hydraulic conductivity function ($L\,T^{-1}$), h is the soil water pressure head (L), x is the lateral coordinate, z is the vertical coordinate (positive downwards), t is time (T), and $WU(h, r, z)$ denotes root water uptake (T^{-1}). WU is computed as follows:

$$WU(h,x,z) = \gamma(h) RDF(x,z) WT_{pot} \quad (3)$$

where $\gamma(h)$ is the soil water stress function (dimensionless) of Feddes et al. (1978), RDF is the normalized root water uptake distribution [L^{-2}], T_{pot} is the potential transpiration rate [$L\,T^{-1}$], and W is the width of the soil surface [L] associated with the transpiration process. In the present study, the root distribution was assumed to be described using the Vrugt et al. (2001) function and to be constant in time (which is a restriction of HYDRUS-2D).

Crop evapotranspiration (ET_c) under the FI treatment was assumed to represent potential crop evapotranspiration since crops under this treatment were well-irrigated (i.e., there was no water stress in the rooting zone since irrigation events were scheduled to always refill soil water content to field capacity), well fertilized, and were treated with pesticides to control weeds, aphids and fungal diseases during both growing seasons. Moreover, the crop achieved its full production when considering the maize yield potential for given climate conditions in the study area. Details about how ET_c was obtained is given in Karandish and Šimůnek (2016).

Measured leaf area index (LAI) was applied to divide ET_c into potential evaporation (E_p) and potential transpiration (T_p) as follows (Belmans et al., 1983):

$$\begin{aligned} E_p &= ET_c e^{-K_{gr}^* LAI} \\ T_p &= ET_c - E_p \end{aligned} \quad (4)$$

where E_p is potential evaporation [$L\,T^{-1}$], T_p is potential transpiration [$L\,T^{-1}$], ET_c is crop evapotranspiration [$L\,T^{-1}$], and K_{gr} is an extinction coefficient for global solar radiation [–]. K_{gr} was set to 0.39 following the suggestions by Ritchie (1972) and Feddes et al. (1978). Estimated values of E_p and T_p were used as input parameters in HYDRUS-2D. Temporal variations of ET_c under different treatments can be found in Karandish and Šimůnek (2016).

The soil hydraulic properties were modeled using the van Genuchten-Mualem constitutive relationships (van Genuchten, 1980). The Galerkin finite element method was used for solving Eq. (3) based on the iterative mass conservative scheme proposed by Celia et al. (1990).

2.2.2. Geometry information and boundary conditions

The domain geometry was defined to represent a typical maize field in which driplines are located between maize rows with a row spacing of 75 cm (Fig. 1b). The two-dimensional transport domain was a rectangle 75 cm wide between two neighboring emitters on either side of one plant (Fig. 1b) and with a soil depth of 80 cm. The soil depth was selected so that the observed maximum rooting depth was situated above this depth. The driplines were considered to be line sources, since the emitter spacing along the driplines was relatively small (i.e., 20 cm in this field investigation). The spatial domain was discretized using unstructured triangular finite element mesh (FEM) defined using 2215 nodes. A non-uniform FEM was generated by HYDRUS-2D with finite element sizes gradually increasing with distance from the emitters. A high nodal density is required in the immediate vicinity of the emitters to accurately model the large spatial gradients in soil water pressure heads caused by infiltrating water (Kandelous et al., 2011). Two soil horizons with different soil hydraulic properties were defined at the 0–20 cm and 20–80 cm soil depths.

Initial conditions were defined based on the field measurements. The time-variable and atmospheric boundary conditions were specified at the soil surface to represent drip irrigation and to apply precipitation, evaporation, and transpiration fluxes, respectively. A free drainage boundary condition was applied along the bottom boundary, allowing for downward drainage. All other remaining boundaries were assigned a no-flow boundary condition.

2.2.3. Model calibration and validation

The sensitivity analysis was carried out to determine how the soil hydraulic parameters affect the HYDRUS-2D simulated SWCs. The sensitivity coefficients for individual parameters were calculated according to Šimůnek and van Genuchten (1996). Thereafter, the most sensitive parameters were optimized in the calibration process. Detailed information about the calibration and validation process can be found in Karandish and Šimůnek (2016).

2.2.4. Multiple Linear Regressions (MLR)

Regression analysis is commonly used to describe quantitative relationships between a response variable and one or more explanatory variables (Tabari et al., 2012). The linear equation in MLR is as follows:

$$Y = \alpha_0 + \alpha_1 X_1 + \alpha_2 X_2 + \cdots + \alpha_n X_n \quad (5)$$

where Y is the dependent variable, $\alpha_0 - \alpha_n$ are the MLR parameters, and $X_1 - X_n$ are the independent variables (Ozbayoglu and Ozbayoglu, 2006).

For all evaluated MLR models, SWC was defined as a dependent variable. First, a Pearson-correlation matrix was established between SWC as a dependent variable and different independent variables. Thereafter, variables which had the highest correlation coefficient with SWC were selected independent variables in the MLR models. The set of independent variables included pan evap-

oration (E), average air temperature (T), crop coefficient (K_c), cumulative growth degree day ($cGDD$), net irrigation depth (In) and water deficit (WD). These parameters were selected since they are easy to obtain and affect SWCs. While T and E are considered to be atmospheric factors, K_c and $cGDD$ are considered to be crop factors. WD and In represent stress conditions in the soil and affect SWCs through root water uptake. WD is calculated as $WD = (\theta_{FC} - \theta_{pwp}) * \alpha$, where, θ_{FC} is the volumetric soil water content at field capacity, θ_{pwp} is the volumetric soil water content at the permanent wilting point and α is a coefficient, which is set to 1, 0.75, and 0.55 for the FI, PRD_{75}, and PRD_{55} treatments, respectively. Eight combinations of input variables were evaluated in this study: (i) E, K_c, and In; (ii) E, K_c, WD, and In; (iii) $cGDD$, E, K_c, and In; (iv) K_c, T, and In; (v) K_c, WD, T, and In; (vi) $cGDD$, K_c, T, and In; (vii) $cGDD$, K_c, and In, and (viii) $cGDD$, K_c, WD, and In.

2.3. Adaptive Neuro-Fuzzy Inference Systems (ANFIS)

Jang (1993) introduced the Adaptive Neuro-Fuzzy Inference Systems method (ANFIS), which combines neural networks and the capabilities of the fuzzy theory (Tang et al., 2010). A popular teaching method in neuro-fuzzy systems is the fuzzy inference system, which uses the hybrid learning algorithms to identify the fuzzy system parameters and to teach the model (Rehman and Mohandes, 2008). The ANFIS model has a five-layer structure (Fig. 2), which is the result of adding the fuzzy logical models to the artificial neural networks:

Layer 1 or Input Layer: In this layer, the membership degree of the nodes entering different fuzzy periods is determined by using the membership functions (MFs). There are numerous kinds of MFs, such as trapezoids, sigmoid, Gaussian, and bell-shaped functions. Two fuzzy sets are considered for each input. The shape of the MFs and the values of their overlapping are optional and determined by Eq. (5):

$$\mu_A(x) = \frac{1}{1 + \left|\frac{x - c_i}{a_i}\right|^{2b_i}} \tag{6}$$

where x is input, and a, b, and c are comparative parameters and the non-linear coefficients, which determine the shape of the MFs. The set of the fuzzy variables is called the S1 set or the left-handed set (LHS). The output values of the first layer show the membership values of ach input for specific MFs.

Layer 2: This layer is the result of multiplying the input values by the nodes, and then finally the firing strength (i.e., weight). For example, for the first node, we have:

$$w_i = \mu_{A_1(x_1)} \mu_{B_1(x_2)} \tag{7}$$

Layer 3: Its nodes normalize the firing strength:

$$\bar{W}_1 = \frac{w_1}{\sum_{i=1}^{n} w_i}, \quad i = 1, 2, \ldots, n \tag{8}$$

where n is the number of nodes in each layer.

Layer 4: This is the terms layer, in which terms are achieved. These terms are the results of operation on the input signals into this layer:

$$Z_1 = \bar{w}_1 f_1 = \bar{w}_1 (p_1 x_1 + q_1 x_2 + r_1) \tag{9}$$

where p_1, q_1, and r_1 are the consequent parameters.

Layer 5: This is the last layer of the net, which includes only one node, and is calculated by adding all input values into its total output:

$$\sum_{i=1}^{n} \bar{w}_i f_i \tag{10}$$

In the structure of the ANFIS model, there are sets of comparative parameters S_1 (the set of fuzzy variables), and consequent parameters S_2. Simulation is correctly performed when both parameters are estimated in a way that minimizes the values of the error function of the model in the training, examination, and validation procedures. There are usually two steps to calculate these parameters. The first step is a forward pass, which considers the static S_1 and S_2 parameters, by using the least square error algorithm. The second step is called a backward pass, which considers that the static S_1 and S_2 are obtained using the Gradient Descent algorithm. These sets of functions, called Epoch, appear at every stage of training (Tabari et al., 2012). By calculating the parameters of the model, the output values of the model are obtained for each arranged couple, which is sent to the model through the training data of the model. The estimated values are compared to the real values in order to calculate the training error function of the ANFIS model. In every step of the Epoch training course, the values of the model parameters change; thus, the values of the training error and the test error of the model vary. The maximum values are selected in a way that the model does not require extra training (Dastirani et al., 2010).

One of the features of every ANFIS model is the type of function considered for the model inputs. In this study, different MFs were employed and different numbers of MFs were tried in each application. The combination of MFs and their numbers giving the minimum errors were selected. Different ANFIS architectures were evaluated using a MATLAB code that included fuzzy logic. Efficient models were first determined for each combination of input variables. Then, the various ANFIS models were tested and obtained results were evaluated using different criteria indices. For both

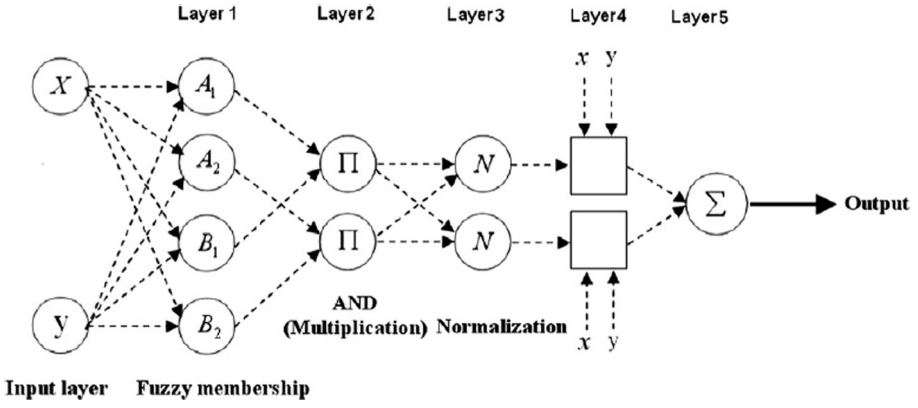

Fig. 2. Schematic of the ANFIS architecture.

ANFIS and SVM models (described below), the same combinations of independent input variables were used as were described above for the MLR models (i.e., eight input combinations involving *E*, *T*, K_c, *WD*, *cGDD*, and *In*).

2.4. Support Vector Machines (SVM)

Introduced by Vapnik (1995), Support Vector Machines (SVM) are a classifier derived from statistical learning theory. The SVM can be used both for classification and regression problems. They can be represented as a two-layer network where the weights are non-linear in the first layer and linear in the second layer (Bray and Han, 2004). The Support Vector Regression (SVR) is used in literature to describe regression with SVM. The regression estimation with SVR is to estimate a function according to a given data set, $\{(x_i,y_i)\}_n$, where x_i denotes the input vector, y_i denotes the output value, and n is the total number of data points (Tabari et al., 2012). The input vectors (x_i) refer to independent variables, whereas the target values (y_i) refer to SWC. The linear regression function uses the following function:

$$f(x) = \omega\phi(x) + b \tag{11}$$

where $\phi(x)$ is a nonlinear function by which x is mapped into a feature space, b and ω are a weight vector and a coefficient, respectively, that should be estimated from the data. A linear regression is performed in a high dimensional feature space via non-linear mapping. The coefficients b and x are estimated by minimizing the sum of the empirical risks (the first term of Eq. (12)) and a complexity term (the second term of Eq. (12)).

$$R = c\sum_{i=1}^{n} L_\varepsilon(f(x_i), y_i)\frac{1}{2}\|\omega\|^2 \tag{12}$$

$$L_\varepsilon(f(x_i), y_i) = \begin{cases} 0 & for |f(x_i) - y_i| < \varepsilon \\ |f(x) - y| - \varepsilon & otherwise \end{cases} \tag{13}$$

where R is the sum of the empirical risks, c is a positive constant (an additional capacity control parameter) that determines the trade-off between the model complexity and the values up to which errors larger than ε are tolerated, ω^2 is the regularization term, which denotes the Euclidean norm, y is the output value, and L_ε is called the e-insensitive loss function that measures the empirical risk and has the advantage of not requiring all input data for describing the regression vector x.

Eq. (12) shows that the loss function is equal to 0 if the difference between the predicted $f(x)$ and the measured value y_i is less than ε. The choice of ε is easier than the choice of c and it is often given as a desired percentage of the output values y_i. So, a non-linear regression function is given by a function that minimizes Eq. (11), subject to Eq. (12), as in the following expression:

$$f(x, \alpha, \alpha^*) = \sum_{i=1}^{n}(\alpha_i - \alpha^*)k(x_i, x) + b \tag{14}$$

Coefficient $\alpha_i\alpha^* = 0$ or $\alpha_i\alpha^* \geqslant 0$ for $i = 1, \ldots, N$ and the kernel function $k(x_i, x)$ describe the inner products in the D-dimensional feature space:

$$k(x, y) = \sum_{i=1}^{D}\phi_j(x)\phi_i(y) \tag{15}$$

It should be mentioned that the features ϕ_j need not be computed; rather what is needed is the kernel function, which is very simple and has a known analytical form. In this study, linear, polynomial, radial basis function, and sigmoid kernels were used. The best kernel was determined by a trial and error process. The coefficients $\alpha_i\alpha^*$ are obtained by maximizing the following form:

$$\begin{aligned} R(\alpha_i\alpha^*) &= -\varepsilon um_{i=1}^{N}(\alpha_i + \alpha^*) + \sum y_i(\alpha^* - \alpha_i) \\ &\quad -\tfrac{1}{2}\sum_{j=1}^{N}(\alpha^* + \alpha_i) \times (\alpha^* + \alpha_i)k(x_i, x_j) \\ subject\ to\ &\sum_{i=1}^{N}(\alpha^* - \alpha_i) = 0 \text{ and } 0 \leqslant \alpha_i\alpha^* \leqslant C \end{aligned} \tag{16}$$

Only a number of coefficients $\alpha_i\alpha^*$ will be different from zero, and the data points associated to them are called support vectors (Mohandes et al., 2004; Kisi and Cimen, 2009; Zhou et al., 2009).

2.5. Correspondence criteria indices

The root mean square error (RMSE), the mean bias error (MBE), the model efficiency (EF) and the coefficient of determination (R) were calculated to provide the quantitative comparison of the correspondence between the predicted and observed data as follows (Parchami-Araghi et al., 2013):

$$RMSE = \sqrt{\frac{\sum_{i=1}^{n}(O_i - P_i)^2}{n}} \tag{17}$$

$$MBE = \frac{\sum_{i=1}^{n}(O_i - P_i)}{n} \tag{18}$$

$$EF = 1 - \frac{\sum_{i=1}^{n}(O_i - P_i)^2}{\sum_{i=1}^{n}(O_i - \overline{O_i})^2} \tag{19}$$

where P_i and O_i are the predicted and observed data, respectively, $\overline{O}$ and $\bar{P}$ are the averages of observed and simulated data, respectively, and n is the number of observations.

3. Results and discussion

The HYDRUS-2D, MLR, ANFIS, and SVM models were evaluated to simulate temporal variations of SWC data during two years and for the FI, PRD_{75}, and PRD_{55} treatments. It should be noted that the SWC results are presented for all methods, except for HYDRUS-2D, in terms of average values for the entire simulation domain in the FI treatment, which is an 80 cm deep rectangle between two neighboring emitters on either side of one plant (as explained in Section 2); and in terms of average values for each sides of the plant in the PRD treatments. Although the results for HYDRUS-2D are presented for every 20 cm soil depth in Table 4 and for different positions of the wetting front in Fig. 3, the average RMSE and MBE values were calculated for the entire soil domain of 0–80 cm by averaging these statistics from individual soil layers.

3.1. HYDRUS-2D

Soil hydraulic properties (i.e., K_s, θ_s, and θ_r) for the two horizons of the soil profile (i.e., 0–20 cm and 20–80 cm soil depths) were optimized for all treatments using the inverse option of HYDRUS-2D that minimizes deviations between the observed and simulated SWCs. Based on the results of the optimization, summarized in Table 3, θ_r was the most sensitive parameter, followed by K_s, for predicting observed soil water contents in the 0–20 cm soil depth. In contrast, for the 20–80 cm soil depth, K_s was the most sensitive parameter. Soil water contents showed less sensitivity to θ_s during the calibration process than to K_s and θ_r.

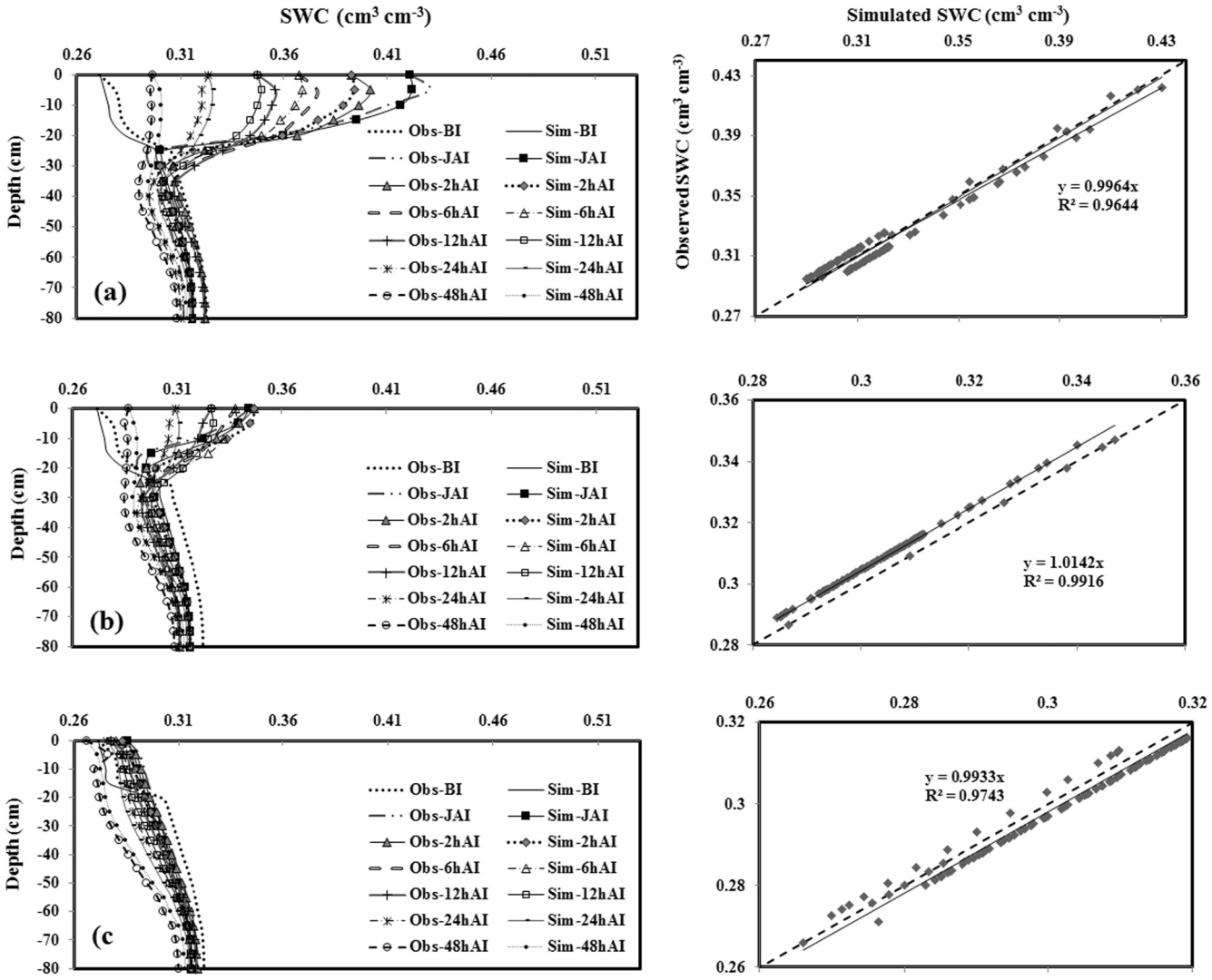

Fig. 3. A comparison of observed and simulated (HYDRUS-2D) soil water contents at 0 (a), 18.75 cm (b), 37.5 cm (c), 56.25 cm (d), and 75 cm (e) distance from the first dripper in the FI treatment (BI and AI denote before and after irrigation, respectively).

Table 3
Measured and optimized soil hydraulic parameters (K_s is the saturated hydraulic conductivity, and θ_r and θ_s are the residual and saturated water contents, respectively).

Treatment	Soil depth (cm)	K_s (cm day^{-1})		θ_s (cm^3 cm^{-3})		θ_r (cm^3 cm^{-3})	
		Optimized	Observed*	Optimized	Observed	Optimized	Observed
FI	0–20	1.3	1.1	0.47	0.45	0.10	0.07
	20–80	1.0	0.80	0.47	0.48	0.07	0.09
PRD_{75}	0–20	1.22	1.05	0.47	0.47	0.10	0.08
	20–80	0.95	0.83	0.47	0.48	0.08	0.08
PRD_{55}	0–20	1.15	1.1	0.47	0.46	0.09	0.06
	20–80	0.90	1.0	0.47	0.47	0.07	0.08

* Observed refers to parameters fitted by RETC to retention curves determined in the laboratory. Only K_s, θ_s, and θ_r were optimized by HYDRUS-2D, while parameters α, l, and n were kept equal to values obtained by RETC.

As an example, a comparison between observed and simulated SWCs during the calibration process for the FI treatment is illustrated in Fig. 3. Good agreement was obtained between observed and simulated SWCs at the sampling points between two neighboring emitters when the optimized soil hydraulic parameters were used during the calibration period. A lower R^2 (0.96–0.97) was obtained for SWCs observed in the vicinity of drippers where SWC variations were higher. Small differences between observed and simulated SWCs can be a consequence of the fact that HYDRUS-2D provides point values of SWCs, while measurements inherently average SWCs over a certain soil volume, in which water contents may vary, especially in the vicinity of emitters (Mguidiche et al., 2015). Similar calibration results were also observed for the PRD_{75} and PRD_{55} treatments, which confirm the high potential of HYDRUS-2D to simulate SWCs.

Daily SWCs for 2011 growing seasons were used to validate HYDRUS-2D (i.e., results are also presented for daily SWCs during the 2010 growing season in Fig. 4 for the visual comparison of

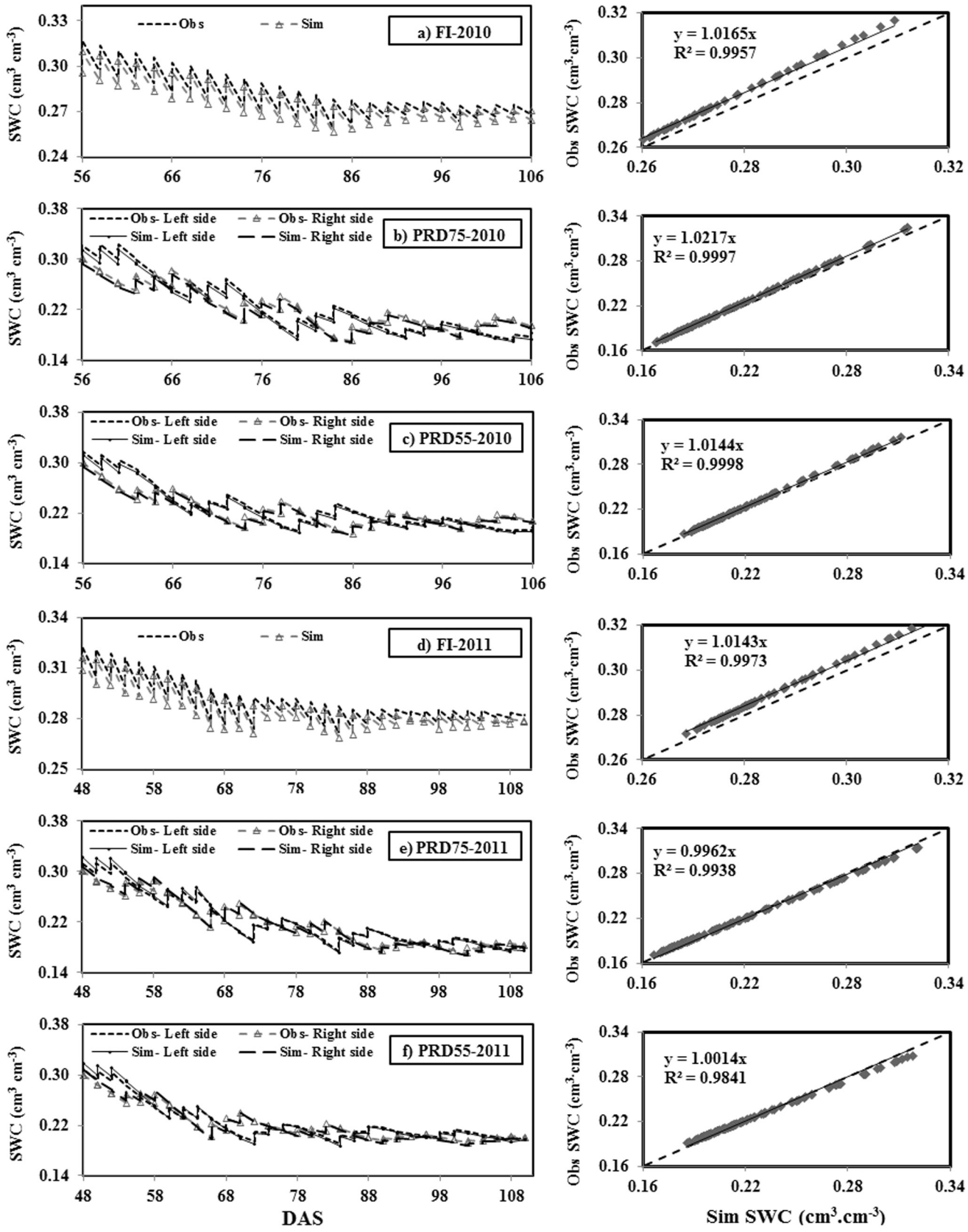

Fig. 4. A comparison of temporal variations of measured and simulated (HYDRUS-2D) average SWCs in the root zone (i.e., 0–80 cm) during the 2010 (calibration) and 2011 (validation) growing seasons for the FI (a and d), PRD_{75} (b and e), and PRD_{55} (c and f) treatments.

Table 4
A comparison of observed and simulated (with HYDRUS-2D) EWDi (an equivalent water depth over four horizons) using criteria indices.

Parameter	Depth (cm)	2010						2011					
		FI		PRD_{75}		PRD_{55}		FI		PRD_{75}		PRD_{55}	
		RMSE* (mm)	MBE (mm)	RMSE (mm)	MBE (mm)	RMSE (mm)	MBE (mm)	RMSE (mm)	MBE (mm)	RMSE (mm)	MBE (mm)	RMSE (mm)	MBE (mm)
EWD_i (mm)	0–20	0.8	1.1	0.73	0.93	0.83	0.83	1.18	0.89	0.82	1.4	0.35	0.45
	20–40	0.85	1.2	0.73	0.91	0.79	0.85	0.38	1.2	0.78	0.95	0.72	0.82
	40–60	0.78	0.85	0.64	0.87	0.81	0.69	0.48	0.8	0.80	1.2	0.60	0.70
	60–80	0.28	0.48	3.69	10	5.84	5.5	0.41	0.75	0.87	0.97	0.51	0.65

* RMSE: Root mean square error, MBE: Mean bias error.

Table 5
Statistical performance evaluation criteria for the MLR models using measured and observed SWCs.

Model	Input variables	RMSE (mm)*	MBE (mm)	EF	Equation**
MLR1	E, K_c, In	25.26	−1.37	0.34	$0.163 + 0.001E + 0.048K_c + 0.003In$***
MLR2	E, K_c, WD, In	12.20	0.34	0.85	$0.19 + 0.000022E + 0.041K_c - 0.03WD + 0.0018In$
MLR3	$cGDD$, E, K_c, In	12.00	3.98	0.86	$0.622–0.0028cGDD + 0.000022E - 0.051K_c + 0.000041In$
MLR4	K_c, T, In	17.13	−3.16	0.71	$0.205 + 0.0511K_c + 0.0015T + 0.0028In$
MLR5	K_c, WD, T, In	12.24	0.18	0.85	$0.18 + 0.056K_c + 0.0000018T - 0.019WD + 0.00185In$
MLR6	$cGDD$, K_c, T, In	13.44	7.14	0.82	$0.65–0.0031cGDD - 0.0702K_c + 0.0000021T + 0.00000014In$
MLR7	$cGDD$, K_c, n	14.78	9.48	0.79	$0.721–0.0025cGDD - 0.042K_c + 0.0018In$
MLR8	$cGDD$, K_c, WD, In	10.46	6.86	0.90	$0.531–0.0028cGDD - 0.0499K_c - 0.065WD + 0.0015In$

* RMSEs and MBEs are calculated for equivalent root zone water depth (EWD_{rz}).
** Equations are for SWCs.
*** DAS: days after sowing (d), K_c: crop coefficient (dimensionless), WD: water deficit (dimensionless), In: irrigation depth (mm), E: evapotranspiration (mm), GDD: growth degree day (°Cd).

the observed and HYDRUS-2D simulated SWCs). Temporal variations of measured and simulated SWCs averaged over the rooting depth (i.e., 0–80 cm) for both growing seasons, as well as the related scatter plots, are displayed in Fig. 4 for all treatments. HYDRUS-2D performed very well in simulating average root zone SWCs and their seasonal trends. Similar results were found in Pang et al. (2000) and Mguidiche et al. (2015), who concluded that HYDRUS-2D is capable of simulating the general trend of SWCs for both homogenous and heterogeneous soils.

The performance of the HYDRUS-2D model in simulating SWCs in terms of RMSE and MBE is summarized in Table 4. RMSE values characterizing differences between observed and simulated SWCs varied between 0.28–1.18 mm for the FI treatment, 0.64–3.69 mm for the PRD_{75} treatment, and 0.35–5.84 mm for the PRD_{55} treatment (the RMSE and MBE values were calculated for equivalent water depths over four different horizons (EWD_i)). In general, higher RMSEs for the FI treatments were obtained for the 0–40 cm surface soil depths, which experience higher variations of SWCs during the growing seasons, than for deeper depths. On the other hand, the highest RMSEs for the PRD treatments were obtained for the 60–80 cm soil depth. A small underestimation of all components of the EWD_i could be observed for all treatments, with MBEs between 0.45–10 mm. Other studies also reported small errors in the simulated components of the seasonal soil water balance using HYDRUS-2D, with RMSEs less than 10 mm (Skaggs et al., 2004; Kandelous and Šimůnek, 2010; Mguidiche et al., 2015).

3.2. The MLR models

Results for the MLR models in terms of predictions of equivalent water depth over root zone (EWD_{rz}) are summarized in Table 5. With respect to RMSE, the MLR8 model with inputs of $cGDD$, K_c, In, and WD had the best performance (RMSE = 10.46 mm, MBE = 6.86, and EF = 0.0.9), followed by the MLR3 (RMSE = 12 mm, MBE = 3.98, and EF = 0.86) and MLR2 (RMSE = 12.2 mm, MBE = 0.34, and EF = 0.85) models. It seems that K_c, which represents the crop growth stage and consequently the crop's water requirements, plays a major role in estimating EWD_{rz} since it always has a higher multiplication coefficient than other input variables. In fact, the higher the root water uptake, the lower the EWD_{rz}.

The input combination of E, K_c, and In (i.e., the MLR1 model) yielded the lowest accuracy in estimating EWD_{rz}. With respect to MBE, MLR7 is the worst model since neither atmospheric factors (i.e., T and E) nor WD are included in its input combination. Generally, underestimation of SWCs is observed for the MLR models, except for MLR1 and MLR4. Overall, differences between observed and simulated SWCs (averaged over the root zone), as illustrated by scatter plots in Fig. 5, indicate a low accuracy of the MLR models in simulating SWCs for different treatments. This low accuracy can be ascribed to the non-linearity of the variably-saturated water flow process and thus the inadequacy of linear relationships between SWCs and selected input parameters.

3.3. The ANFIS and SVM models

Table 6 provides the final architectures of various ANFIS models and the performance statistics for the training phase. Two membership functions (MFs) were found to be sufficient for simulating EWD_{rz} with the ANFIS models except for ANFIS1, for which five MFs led to the best results. The increase in the number of MFs not only does not provide any significant improvements in the results, but also increases the number of parameters that need to be optimized. Because of that, the number of MFs should be kept as low as possible (Ozger and Yıldırım, 2008). Except for ANFIS4, the generalized, bell-shaped built-in (Gb) and Gaussian combination (Gus2) membership functions were the best MFs for all ANFIS models. For ANFIS4, the Gaussian curve built-in (Gus1) function led to the lowest error when simulating EWD_{rz}.

With respect to RMSE, the ANFIS8 model, with inputs of $cGDD$, K_c, WD, and In, had the best performance in simulating EWD_{rz}

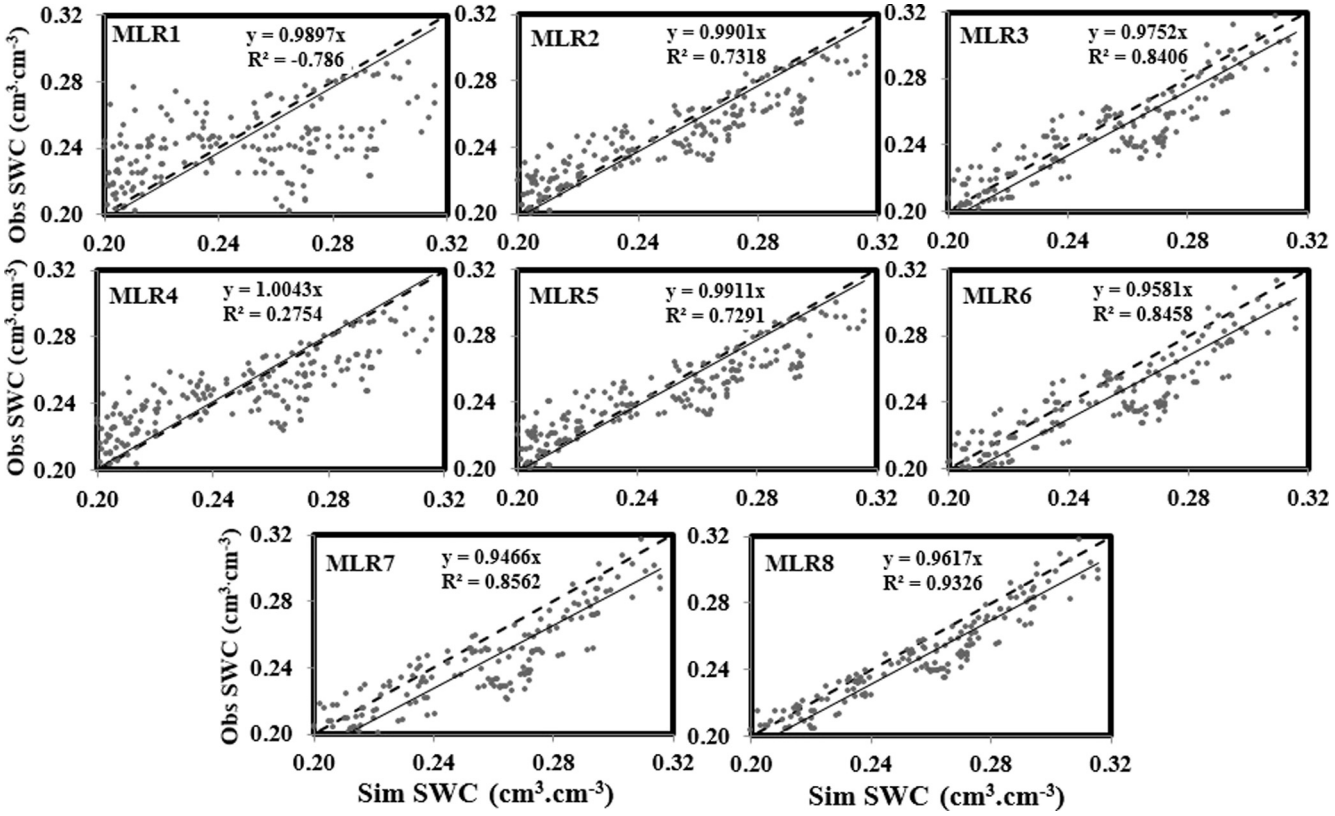

Fig. 5. Scatter plots between observed and simulated SWCs (averaged over the root zone) for the MLR models.

Table 6
The final architecture and performance statistics of the ANFIS models for the testing phase. The same combination of input variables were used in the ANFIS and MLR models (see Table 5).

Model	Input variables	Best MF*	NMF	RMSE (mm)**	MBE (mm)	EF
ANFIS1	*E*, K_c, *In*	Gb	5	22.45	2.61	0.45
ANFIS2	*E*, K_c, *WD*, *In*	Gb	2	4.73	0.03	0.98
ANFIS3	*cGDD*, *E*, K_c, *In*	Gus2	2	3.21	0.66	0.99
ANFIS4	K_c, *T*, *In*	Gus1	2	8.17	0.40	0.93
ANFIS5	K_c, *WD*, *T*, *In*	Gb	2	4.87	−0.23	0.98
ANFIS6	*cGDD*, K_c, *T*, *In*	Gb	2	2.92	0.01	0.99
ANFIS7	*cGDD*, K_c, *In*	Gus2	2	2.71	0.02	0.99
ANFIS8	*cGDD*, K_c, *WD*, *In*	Gus2	2	1.67	−0.11	1.00

* MF: Membership function, NMF: Number of membership function, Gb: Generalized bell-shaped built-in MF, Gus1: Gaussian curve built-in MF, Gus2: Gaussian combination MF.

** RMSEs and MBEs are calculated for equivalent root zone water depth (EWD_{rz}).

(RMSE = 1.67 mm, MBE = −0.11 mm, and EF = 1), and ANFIS7 ranked second (RMSE = 2.71 mm, MBE = 0.02 mm, and EF = 0.99). ANFIS6, with inputs of *cGDD*, K_c, *GDD*, and *In*, ranked third. In contrast, ANFIS1, with input parameters K_c, *E*, and *In*, had the highest error when simulating EWD_{rz} (RMSE = 22.45, MBE = 2.61, and EF = 0.45). Based on the results summarized in Table 6, it seems that crop parameters and factors representing soil stresses play a more important role in temporal variations of EWD_{rz}, compared to atmospheric parameters such as *T* and *E*. As discussed in the literature, crop factors are the most dominant factors, controlling root water uptake under stress conditions, which consequently controls SWCs (Allen et al., 1998).

As shown in Table 6, all ANFIS models underestimated EWD_{rz}, except for ANFIS5 and ANFIS8, which slightly overestimated EWD_{rz}. However, a visual inspection of scatter plots in Fig. 6, comparing observed and ANFIS-estimated SWCs (averaged over the root zone), clearly indicates the high potential of the ANFIS modeling. Notice the high values of R^2 in Fig. 6 for several ANFIS models.

The SVM models were similarly implemented using a MATLAB code. First, different SVM architectures were tried. Once the appropriate model structures were determined for each combination of input variables, the resulting SVM models were tested against the experimental dataset, and the results were compared using the performance statistics (Table 7). In the SVM modeling, an appropriate choice of kernels allows the data to become separable in the feature space despite being non-separable in the original space. This allows one to obtain non-linear algorithms from algorithms previously restricted to handling linearly separable data sets (Bray and Han, 2004). Here, the radial basis function was the best kernel for all SVM models.

With respect to RMSE, the SVM8 model, with RMSE = 1.9 mm, MBE = 0.7 mm, and EF = 1, had the best performance in simulating EWD_{rz}, followed by SVM3 (RMSE = 2.44 mm, MBE = 0.28 mm, and EF = 0.99) and SVM7 (RMSE = 2.66 mm, MBE = 0.15 mm, and EF = 0.99). These three models had nearly the same performance statistics and thus the selection of one of these models over the

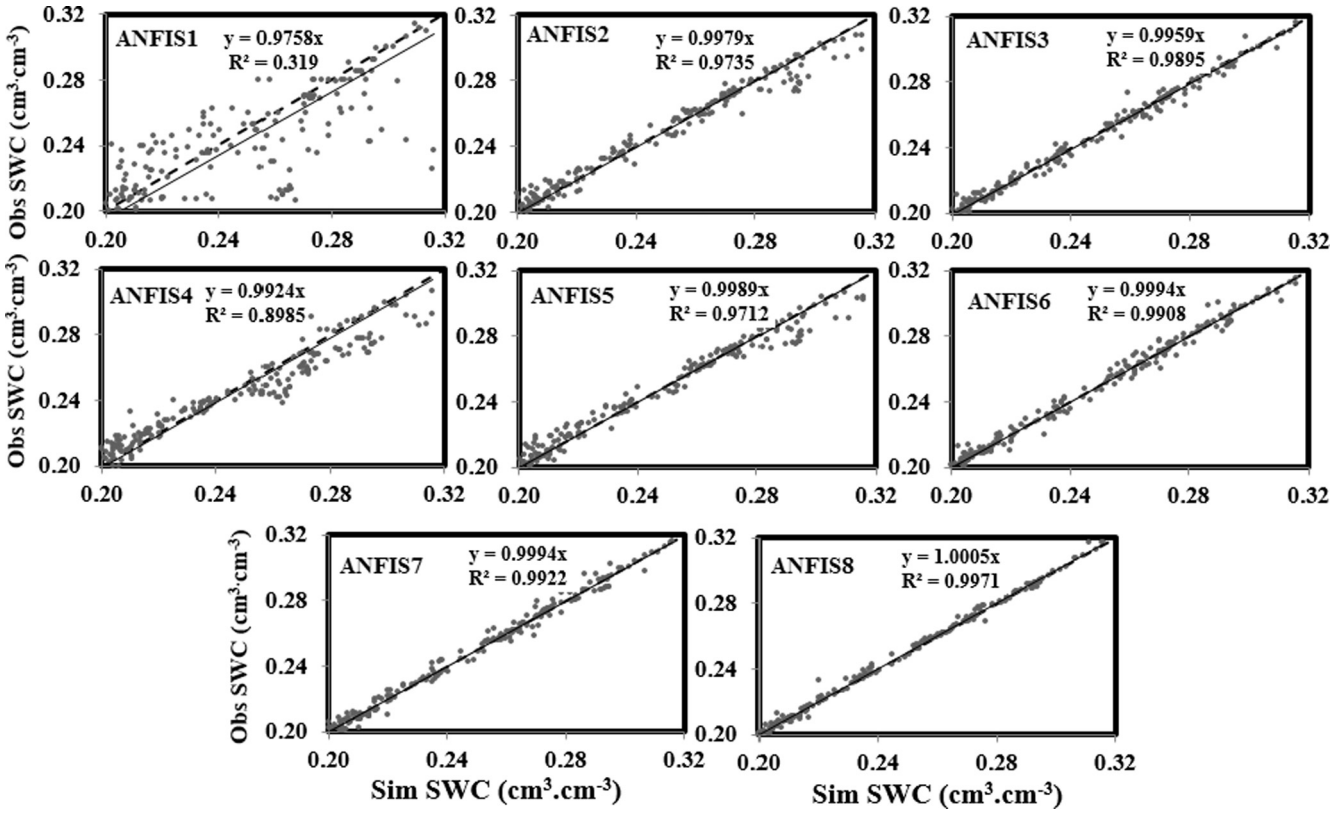

Fig. 6. Scatter plots between observed and simulated SWCs (averaged over the root zone) for the ANFIS models.

Table 7
The final architecture and performance statistics of the SVM models for the testing phase. The same combination of input variables were used in the SVM and MLR models (see Table 5).

Model	Input variables	Best Kernel	RMSE (mm)*	MBE (mm)	EF
SVM1	*E*, K_c, *In*	Radial Basis Function	21.33	2.39	0.51
SVM2	*E*, K_c, *WD*, *In*	Radial Basis Function	3.96	0.43	0.98
SVM3	*cGDD*, *E*, K_c, *In*	Radial Basis Function	2.44	0.28	0.99
SVM4	K_c, *T*, *In*	Linear Function	8.45	0.45	0.93
SVM5	K_c, *WD*, *T*, *In*	Radial Basis Function	4.75	0.37	0.98
SVM6	*cGDD*, K_c, *T*, *In*	Radial Basis Function	3.05	0.21	0.99
SVM7	*cGDD*, K_c, *In*	Radial Basis Function	2.66	0.15	0.99
SVM8	*cGDD*, K_c, *WD*, *In*	Radial Basis Function	1.90	0.27	1.00

* RMSEs and MBEs are calculated for equivalent root zone water depth (EWD_{rz}).

other should be dependent upon available data. Since pan evaporation (*E*) is not always available for all weather stations, the SVM8 and SVM7 models may be easier to use when limited data are available. SVM6, with RMSE = 3.05 mm, MBE = 0.21 mm, and EF = 0.99, also had an acceptable accuracy for estimating EWD_{rz}. Similar to the MLR and ANFIS models, the combination of *E*, K_c, and *In* for SVM1 led to the lowest accuracy in simulating EWD_{rz} (RMSE = 21.33 mm, MBE = 2.39 mm, and EF = 0.51). However, the scatter plots between observed and simulated SWCs (again, averaged over the root zone) and their high R^2 demonstrate the high potential of the SVM modeling (Fig. 7).

3.4. Comparison of different models

A comparison of observed SWCs and SWCs estimated using the MLR8, ANFIS8, and SVM8 models for the FI, PRD_{75}, and PRD_{55} treatments in 2010 is illustrated in Fig. 8 in the form of time series and scatter plots. It should be noted that these particular models had the best performance in their groups. Regardless of the type of model, a better performance was found for the stressed conditions (i.e., PRD_{75} and PRD_{55} treatments) than for the unstressed conditions with full irrigation. This result is contrary to HYDRUS-2D, which had better results for the FI treatment. Negative bias is also obvious for almost all days during the simulation process. Furthermore, a visual inspection of Fig. 8 shows that the ANFIS and SVM models had a better performance than the MLR models for all treatments, which is also reflected by the R^2 index. These models very well reproduced not only the temporal variations, but also the actual daily values of SWCs. Especially, the response of the MLR8 model to irrigation events is less dynamic than observed. This is especially visible for the FI treatment and the wetted sides of the PRD treatments. This documents that the MLR8 model could not well describe non-linear changes in SWCs during irrigation events. This also confirms the RMSE, MBE, and EF statistics given in Tables 5–7.

The performance of different modeling approaches to predict EWD_{rz} is ranked in Table 8 based on the RMSE statistics. Being physically based, the HYDRUS-2D model ranked first with respect

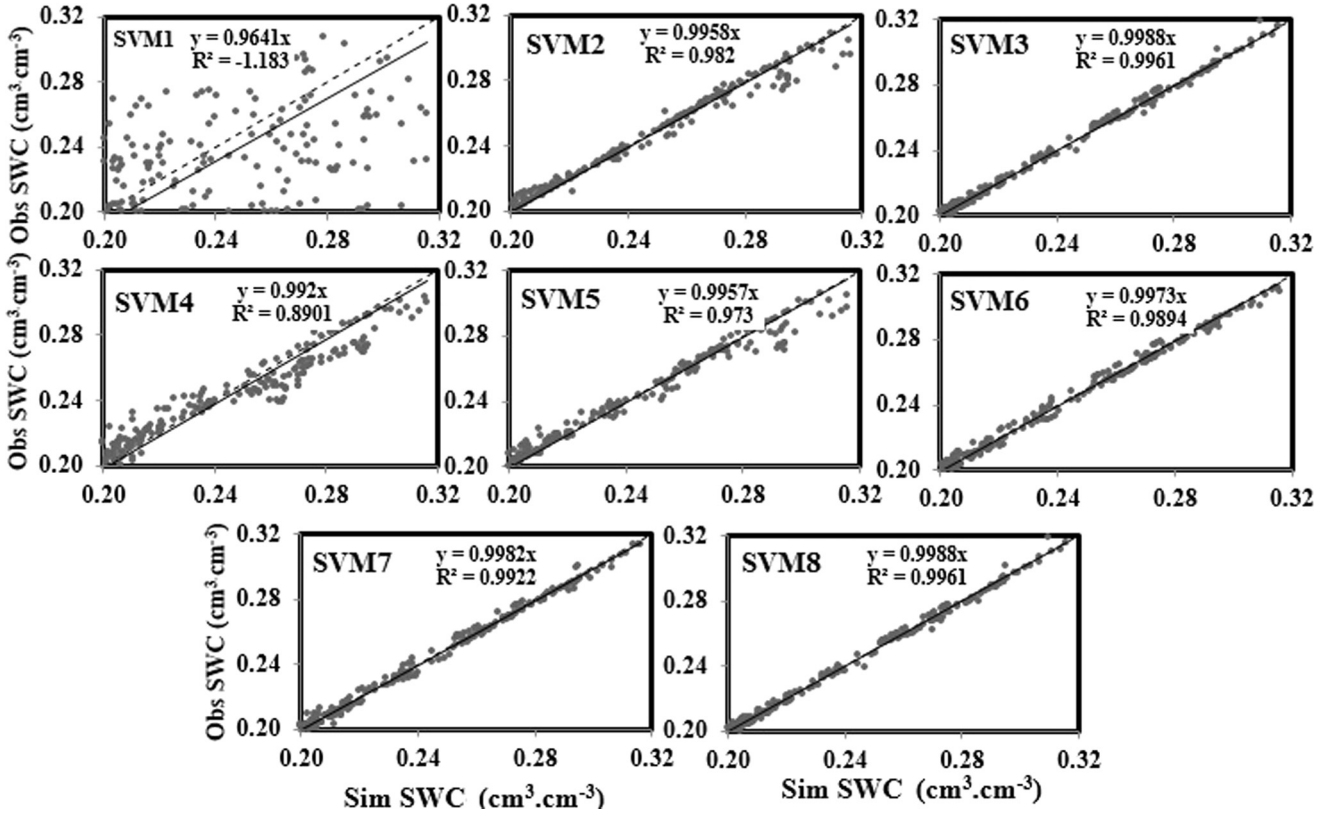

Fig. 7. Scatter plots between observed and simulated SWCs (averaged over the root zone) for the SVM models.

to RMSE. Previous studies have also demonstrated the high potential of HYDRUS-2D for simulating SWCs (e.g., Cote et al., 2003; Ajdary et al., 2007; Rahil, 2007; Crevoisier et al., 2008; Siyal and Skaggs, 2009; Mubarak, 2009; Tafteh and Sepaskhah, 2012). A high accuracy of HYDRUS-2D is to be expected since it is a physically based model that solves numerically by means of the finite element method the Richards equation, which describes the highly non-linear, variably-saturated water flow in soils. This approach requires knowledge of the soil water retention curve and the hydraulic conductivity function, which are rarely known.

Table 8 shows that the ANFIS8 model ranked second (RMSE = 1.67 mm, MBE = −0.11 mm, and EF = 1.00) with respect to the RMSE index, followed by the SVM8 (RMSE = 1.9 mm, MBE = 0.27 mm, and EF = 1.00), SVM3 (RMSE = 2.44 mm, MBE = 0.28 mm, and EF = 0.99) and SVM7 (RMSE = 2.66 mm, MBE = 0.15 mm, and EF = 0.99) models. These models are then followed by ANFIS7 and ANFIS6, and further by SVM6, ANFIS3, SVM2, ANFIS2, SVM5, ANFIS5, ANFIS4 and SVM4. Overall, 14 best performing models for the estimation of EWD_{rz} under stressed conditions were the ANFIS and SVM models, which performed far better than the MLR models. Exceptions were the SVM1 and ANFIS1 models, which by ignoring the *WD* parameter had lower efficiency in estimating EWD_{rz}, especially under stressed conditions. Such results demonstrated that the performance of the ANFIS and SVM models is highly dependent on the selected input datasets. Table 8 shows that the MLR models occupy the last places in terms of their performance in simulating EWD_{rz}. Using the MLR4 model with input parameters of K_c, *GDD*, and *In* led to the worst results.

The ANFIS models combine the transparent linguistic representation of a fuzzy system with the learning ability of ANN. Therefore, they can be trained to perform an input/output mapping similar to ANN while providing an additional benefit of being able to consider a set of rules on which the model is based. This provides a further insight into the process being modeled (Sayed et al., 2003).

The main advantage of using the SVM models is their flexibility and ability to model non-linear relationships. Furthermore, the SVM training process always seeks a global optimized solution and avoids over-fitting, which eventually leads to a better general performance than the ANN models. The SVM models are able to select the key vectors in the training process, which includes support vectors and automatically removes the non-support vectors from the model. This helps the model cope well with noisy conditions. The main disadvantage of the SVM technique is that it has no physical basis. In addition, the SVM approach can only be used when the training dataset is available (Bray and Han, 2004; Zhou et al., 2009; Kisi and Cimen, 2009).

3.5. A further assessment of different models

The performance of different models was reevaluated using the observed SWCs data from 2011. The results of the statistical comparisons between the HYDRUS-2D, MLR, ANFIS, and SVM models are summarized in Table 9, where models are ranked with respect to the RMSE index. Similar to 2010, the best performance criteria for simulating EWD_{rz} were obtained by HYDRUS-2D with RMSE = 0.66 mm, MBE = 0.81 mm, and EF = 0.99. Thereafter, the SVM and ANFIS models generally provided more accurate EWD_{rz} estimations compared to the MLR models. However, the SVM1 and ANFIS1 models performed slightly worse than the MLR models. Overall, Table 9 indicates that the 15 best models for simulating EWD_{rz} in 2011, apart from HYDRUS-2D, were the ANFIS and SVM models, similar to 2010. A visual inspection of observed and simulated SWC time series in Fig. 9 also demonstrated better performance of the ANFIS and SVM models compared to the MLR models. This validation demonstrates that these models could be

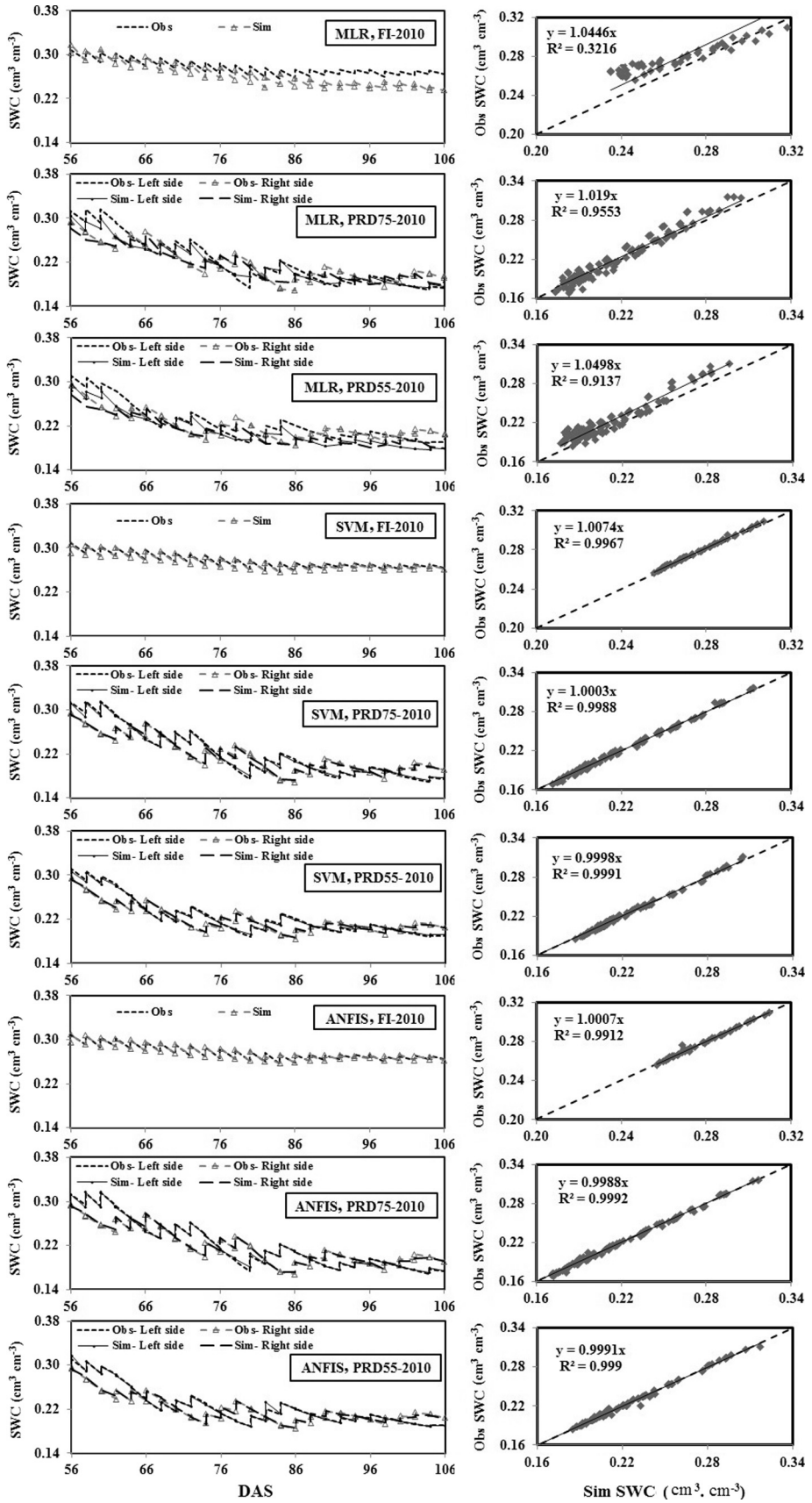

Fig. 8. Average observed and estimated SWCs over the rooting depth (0–80 cm) using the MLR3, SVM3, and ANFIS8 models for different treatments in 2010.

Table 8
Summary of the ranking of selected models (based on the testing phase in 2010).

Rank*	Model	Considered parameters**	RMSE (mm)***	MBE (mm)	EF
1	HYDRUS-2D	physically-based model	1.02	1.45	0.99
2	ANFIS8	*cGDD*, K_c, *WD*, *In*	1.67	−0.11	1.00
3	SVM8	*cGDD*, K_c, *WD*, *In*	1.90	0.27	1.00
4	SVM3	*cGDD*, *E*, K_c, *In*	2.44	0.28	0.99
5	SVM7	*cGDD*, K_c, *In*	2.66	0.15	0.99
6	ANFIS7	*cGDD*, K_c, *In*	2.71	0.02	0.99
7	ANFIS6	*cGDD*, K_c, *T*, *In*	2.92	0.01	0.99
8	SVM6	*cGDD*, K_c, *T*, *In*	3.05	0.21	0.99
9	ANFIS3	*cGDD*, *E*, K_c, *In*	3.21	0.66	0.99
10	SVM2	*E*, K_c, *WD*, *In*	3.96	0.43	0.98
11	ANFIS2	*E*, K_c, *WD*, *In*	4.73	0.03	0.98
12	SVM5	K_c, *WD*, *T*, *In*	4.75	0.37	0.98
13	ANFIS5	K_c, *WD*, *T*, *In*	4.87	−0.23	0.98
14	ANFIS4	K_c, *T*, *In*	8.17	0.40	0.93
15	SVM4	K_c, *T*, *In*	8.45	0.45	0.93
16	MLR8	*cGDD*, K_c, *WD*, *In*	10.46	6.86	0.90
17	MLR3	*cGDD*, *E*, K_c, *In*	12.00	3.98	0.86
18	MLR2	*E*, K_c, *WD*, *In*	12.20	0.34	0.85
19	MLR5	K_c, *WD*, *T*, *In*	12.24	0.18	0.85
20	MLR6	*cGDD*, K_c, *T*, *In*	13.44	7.14	0.82
21	MLR7	*cGDD*, K_c, *In*	14.78	9.48	0.79
22	MLR4	K_c, *T*, *In*	17.13	−3.16	0.71
23	SVM1	*E*, K_c, *In*	21.33	2.39	0.51
24	ANFIS1	*E*, K_c, *In*	22.45	2.61	0.45
25	MLR1	*E*, K_c, *In*	25.26	−1.37	0.34

* Different models are ranked with respect to RMSE.
** *DAS*: days after planting (d), K_c: crop coefficient (dimensionless), *WD*: water deficit (dimensionless), *In*: irrigation depth (mm), *E*: evapotranspiration (mm), *GDD*: growth degree day (°C).
*** RMSEs and MBEs are calculated for equivalent root zone water depth (EWD_{rz}). The RMSE values for HYDRUS-2D were obtained by averaging the values for all individual soil layers which are given in Table 4

Table 9
RMSEs, MBEs and EFs for the selected models during the validation phase, i.e., the 2011 growing season.

Rank*	Model	Considered parameters**	RMSE (mm)**	MBE (mm)	EF
1	HYDRUS2D	Physically-based model	0.66	0.81	0.99
2	SVM8	*cGDD*, K_c, *WD*, *In*	1.27	0.07	1.00
3	ANFIS8	*cGDD*, K_c, *WD*, *In*	1.82	−0.07	1.00
4	SVM3	*cGDD*, *E*, K_c, *In*	2.27	−0.19	1.00
5	ANFIS6	*cGDD*, K_c, *T*, *In*	2.36	0.00	1.00
6	SVM7	*cGDD*, K_c, *In*	2.37	−0.28	1.00
7	ANFIS7	*cGDD*, K_c, *In*	2.46	−0.17	1.00
8	ANFIS3	*cGDD*, *E*, K_c, *In*	2.48	−0.15	1.00
9	SVM6	*cGDD*, K_c, *T*, *In*	2.59	−0.40	0.99
10	SVM2	*E*, K_c, *WD*, *In*	4.40	−0.03	0.99
11	SVM5	K_c, *WD*, *T*, *In*	4.52	0.38	0.98
12	ANFIS2	*E*, K_c, *WD*, *In*	5.02	−0.11	0.98
13	ANFIS5	K_c, *WD*, *T*, *In*	5.84	0.40	0.97
14	ANFIS4	K_c, *T*, *In*	8.75	0.45	0.93
15	SVM4	K_c, *T*, *In*	9.88	3.07	0.91
16	MLR2	*E*, K_c, *WD*, *In*	13.41	−0.61	0.86
17	MLR5	K_c, *WD*, *T*, *In*	13.59	1.65	0.85
18	MLR3	*cGDD*, *E*, K_c, *In*	16.09	9.72	0.81
19	MLR8	*cGDD*, K_c, *WD*, *In*	16.73	14.01	0.83
20	MLR6	*cGDD*, K_c, *T*, *In*	17.01	10.65	0.79
21	MLR4	K_c, *T*, *In*	19.32	−3.58	0.70
22	MLR7	*cGDD*, K_c, *In*	21.76	17.27	0.64
23	SVM1	*E*, K_c, *In*	26.32	5.71	0.36
24	ANFIS1	*E*, K_c, *In*	26.32	5.71	0.36
25	MLR1	*E*, K_c, *In*	26.32	5.71	0.36

The RMSE values for HYDRUS-2D were obtained by averaging the values for all individual soil layers which are given inTable 4
* Different models are ranked with respect to RMSE.
** RMSEs and MBEs are calculated for equivalent root zone water depth (*EWDrz*).

useful substitutes for HYDRUS-2D for optimizing the management of water resources under stressed conditions and with limited data availability in agriculture.

3.6. Uncertainty analysis

Predictions of SWCs immediately before irrigation events are more important for the purpose of irrigation scheduling than of those at other times. Therefore, errors in SWCs and their associated uncertainties before and after irrigation events were estimated with different models separately (Fig. 10). Absolute errors in estimated SWCs immediately before irrigation events using the MLR, ANFIS, SVM, and HYDRUS-2D models ranged between 1.3–17.5%, 0.4–10, 0.2–10.5%, and 1.1–2.8%, respectively. For times after irrigation events, the MLR, ANFIS, SVM, and HYDRUS-2D models estimated SWCs with errors

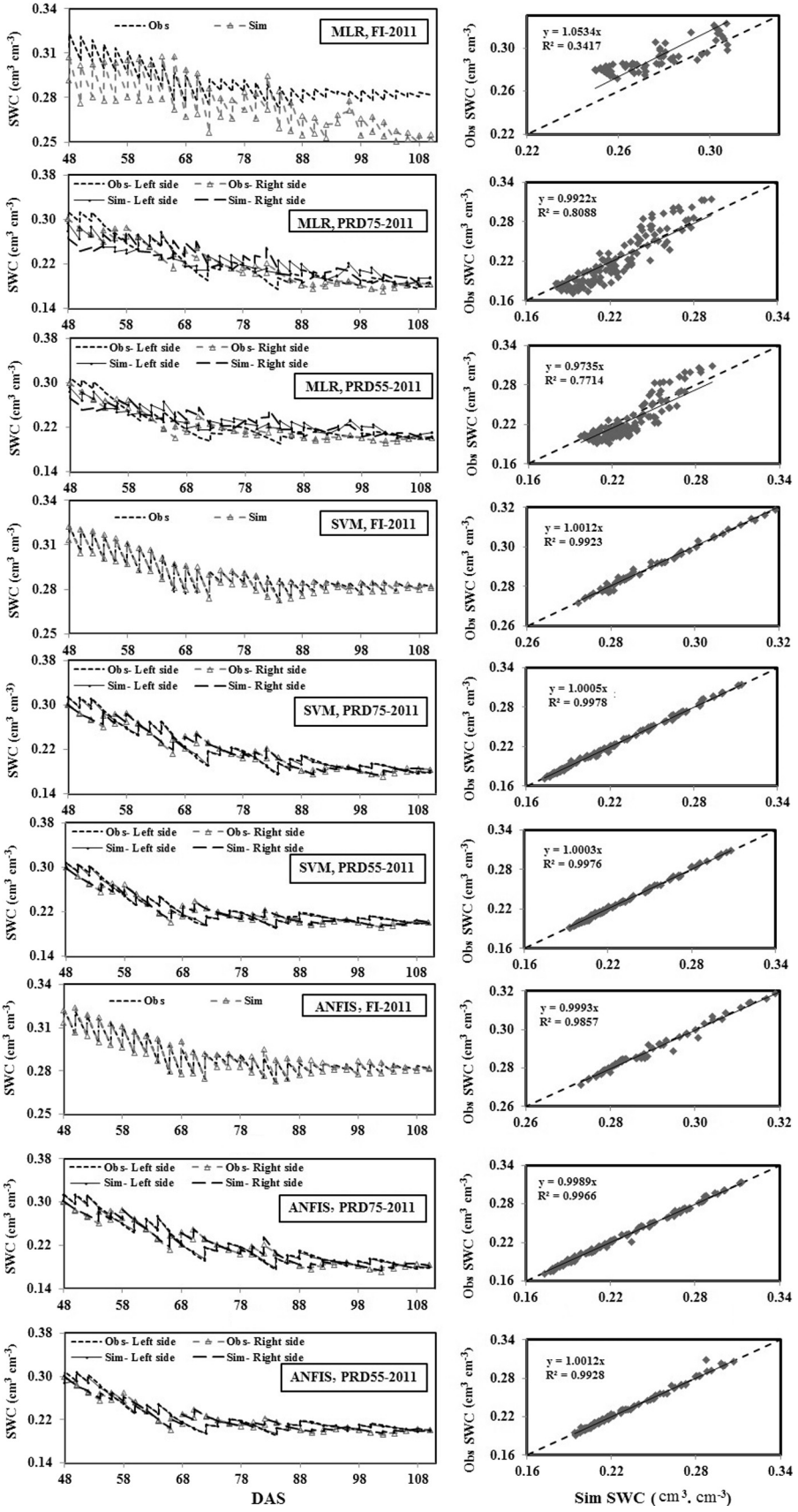

Fig. 9. SWC values observed and estimated using the MLR3, SVM8, and ANFIS6 models for different treatments in 2011.

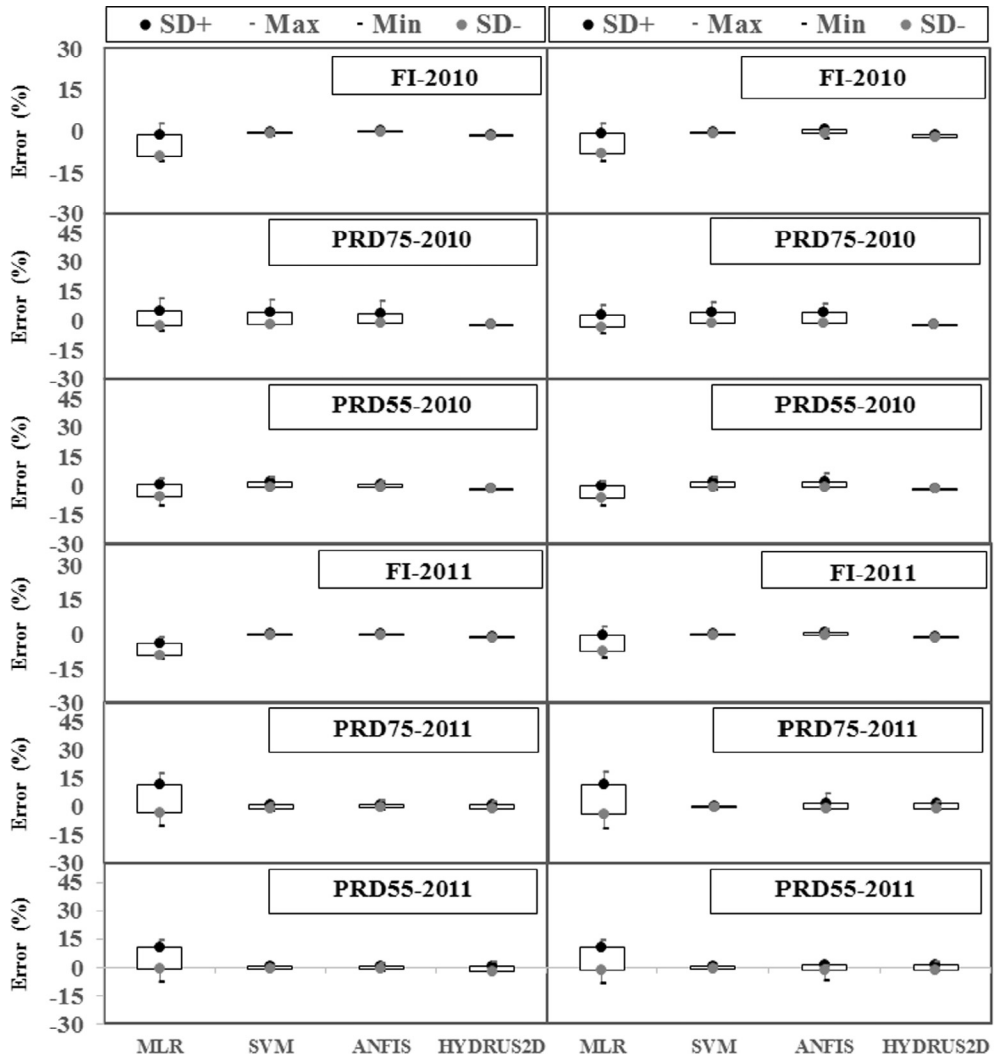

Fig. 10. Errors in estimating SWCs with different models for times immediately before (left) and after (right) irrigation events (Min, Max, and SD denote the minimum, maximum, and standard deviation, respectively).

between 1.7–17.7%, 0.7–8.2%, 0.3–8.7%, and 1.1–3.1%, respectively.

Fig. 10 shows that the results simulated by HYDRUS-2D have a lower uncertainty domain of estimated SWCs than those obtained by the other models and are thus more reliable. Even though the ANFIS and SVM models have absolute errors that are similar to those obtained by HYDRUS-2D, they predict SWCs both before and after irrigation events with higher uncertainties than HYDRUS-2D. Nevertheless, the ANFIS and SVM models performed much better than the MLR models in estimating SWCs and associated uncertainties. It can be concluded that although HYDRUS-2D predictions of temporal variations of SWCs in the root zone are superior to those made by the ANFIS and SVM models, these models can be reliably used for predicting SWCs when there is a lack of data required by HYDRUS-2D.

4. Conclusions

Since agriculture is known to be the biggest consumer of fresh water, sustainable management of water resources for irrigation use has become an important goal at the basin scale worldwide. In this regard, modeling tools for a quick estimation of SWCs and for determining the real crop water demand, especially under new water-saving irrigation strategies, will help farmers improve the water and crop productivity. In this regard, introducing efficient methods for estimating SWCs when only limited information is available would be useful for irrigation scheduling, even in the planning stage when the possible effects of new water-saving irrigation strategies are evaluated. Therefore, in this research, the possibility of indirect estimation of SWCs under water stress conditions was investigated by means of both numerical and machine-learning models, including the HYDRUS-2D, MLR, ANFIS, and SVM models, and using a dataset from a two-year field investigation.

Being a physically-based model, HYDRUS-2D ranked first in simulating time series of SWCs at the field scale for selected irrigation strategies. However, both ANFIS and SVM models could be successfully used for predicting SWCs when there is a lack of input data required by HYDRUS-2D. When suitable input datasets selected based on the correlation analysis were available, these models estimated SWCs with an accuracy that approached the physically based model (Tables 8 and 9). In addition, these models performed especially well compared to HYDRUS-2D for water stressed conditions, although less well for conditions with full irrigation.

Using simple atmospheric data (E, T), crop parameters ($cGDD$, K_c), and stress descriptor parameters (In, WD), the ANFIS, and SVM models showed a high potential for modeling SWCs with

acceptable errors. Therefore, when suitable input datasets are available, the ANFIS and SVM models can be used for irrigation scheduling and for management of agricultural water resources. However, these models have to first be trained using a training dataset that should include as many data and as many conditions as possible so that they can take into account unusual events and obtain good accuracy in their predictions. The models introduced in this research could be used in a wide range of applications since they were developed using only simple input parameters, which could be easily determined even in projects with limited resources.

References

Ahmad, S., Simonovic, S.P., 2005. An artificial neural network model for generating hydrograph from hydro-meteorological parameters. J. Hydrol. 315, 236–251. http://dx.doi.org/10.1016/j.jhydrol.2005.03.032.

Ajdary, K., Singh, D.K., Singh, A.K., Khanna, M., 2007. Modeling of nitrogen leaching from experimental onion field under drip fertigation. Agric. Water Manage. 89, 15–28.

Allen, R.G., Pereira, L.S., Howell, T.A., Jensen, M.E., 2011. Evapotranspiration information reporting: I. Factors governing measurement accuracy. Agr. Water Manag. 98, 899–920.

Allen, R.G., Pereira, L.S., Raes, D., Smith, M., 1998. Crop evapotranspiration guide Lines for computing crop water requirements, Irrigation and Drainage Paper 56, Rome, Italy, p. 300.

Armstrong, A.C., Legros, J.P., Voltz, M., 1996. ACCESS-II: Detailed model for crop growth and water conditions. Int. Agrophys. 10 (3), 171–184.

Asefa, T., Kemblowski, M., McKee, M., Khalil, A.F., 2006. Multi-time scale stream flow predictions: the support vector machines approach. J. Hydrol. 318, 7–16. http://dx.doi.org/10.1016/j.jhydrol.2005.06.001.

Belmans, C., Wesseling, J.G., Feddes, R.A., 1983. Simulation model of the water balance of a cropped soil: SWATRE. J. Hydrol. 63 (3), 271–286.

Billib, M., Bardowicks, K., Arumi, J.L., 2009. Integrated water resources management for sustainable irrigation at the basin scale. Chilean J. Agric. Res. 69 (1), 69–80.

Bray, M., Han, D., 2004. Identification of support vector machines for runoff modeling. J. Hydroinf. 6 (4), 265–280.

Cameira, M.R., Fernando, R.M., Pereira, L.S., 2003. Monitoring water and NO_3-N in irrigated maize fields in the Sorraia Watershed, Portugal. Agric. Water Manage. 60, 199–216. http://dx.doi.org/10.1016/S0378-3774(02)00175-0.

Celia, M.A., Bouloutas, E.T., Zarba, R.L., 1990. A general mass-conservative numerical solution for the unsaturated flow equation. Water Resour. Res. 26, 1483–1496.

Cote, C.M., Bristow, K.L., Charlesworth, P.B., Cook, F.J., Thorburn, P.J., 2003. Analysis of soil wetting and solute transport in subsurface trickle irrigation. Irrigation Sci. 22, 143–156.

Crevoisier, D., Popova, Z., Mailhol, J.C., Ruelle, P., 2008. Assessment and simulation of water and nitrogen transfer under furrow irrigation. Agric Water Manage. 95, 354–366.

Dai, X., Huo, Z., Wang, H., 2011. Simulation for response of crop yield to soil moisture and salinity with artificial neural network. Field Crops Res. 121, 441–449. http://dx.doi.org/10.1016/j.fcr.2011.01.016.

Dastirani, M.T., Moghadamnia, A., Piri, J., Rico-Ramirez, M., 2010. Application of ANN and ANFIS models for reconstructing missing flow data. Environ. Monit. Asses. 166, 421–434.

Deng, J., Chen, X., Du, Z., Zhang, Y., 2011. Soil water simulation and predication using stochastic models based on LS-SVM for red soil region of China. Water Resour. Manage. 25, 2823–2836. http://dx.doi.org/10.1007/s11269-011-9840-z.

Dorji, K., Behboudian, M.H., Zegbe-Domínguez, J.A., 2005. Water relations, growth, yield, and fruit quality of hot pepper under deficit irrigation and partial rootzone drying. Sci. Hortic. 104, 137–149.

Dry, P.R., Loveys, B.R., 1998. Factors influencing grapevine vigor and the potential for control with partial rootzone drying. Aust. J. Grape Wine Res. 4, 140–148.

Dry, P.R., Loveys, B.R., During, H., 2000. Partial drying of the root zone of grape. 2. Changes in the patterns of root development. Vitis 39, 9–12.

Elshorbagy, A., Parasuraman, K., 2008. On the relevance of using artificial neural networks for estimating soil moisture content. J. Hydrol. 362, 1–18. http://dx.doi.org/10.1016/j.jhydrol.2008.08.012.

Feddes, R.A., Kowalik, P.J., Zaradny, H., 1978. Simulation of field water use and crop yield. In: Simulation Monographs, Pudoc, Wageningen.

Fernández, J.E., Sławiński, C., Moreno, F., Walczak, R.T., Vanclooster, M., 2002. Simulating the fate of water in a soil-crop system of a semi-arid Mediterranean area with the WAVE 2.1 and the EURO-ACCESS-II models. Agric Water Manage. 56, 113–129. http://dx.doi.org/10.1016/S0378-3774(02)00009-4.

Jang, J.S.R., 1993. ANFIS: adaptive-network-based fuzzy inference system. IEEE Trans. Syst., IEET SYST Man Cyb. 23 (3), 665–685. http://dx.doi.org/10.1109/21.256541.

Jiang, H., Cotton, W.R., 2004. Soil moisture estimation using an artificial neural network: a feasibility study. Can. J. Rem. Sens. 30, 827–839. http://dx.doi.org/10.5589/m04-041.

Kandelous, M.M., Šimůnek, J., 2010. Numerical simulations of water movement in a subsurface drip irrigation system under field and laboratory conditions using HYDRUS-2D. Agric. Water Manage. 97, 1070–1076.

Kandelous, M.M., Šimůnek, J., van Genuchten, M.Th., Malek, K., 2011. Soil water content distribution between two emitters of a subsurface drip irrigation system. Soil Sci. Soc. Am. J. 75 (2), 488–497.

Kang, S., Zhang, J., 2004. Controlled alternate partial root-zone irrigation: its physiological consequences and impact on water use efficiency. J. Exp. Bot. 55 (407), 2437–2446.

Karandish, F., Šimůnek, J., 2016. A field-modeling study for assessing temporal variations of soil-water-crop interactions under water-saving irrigation strategies. Agric. Water Manage. 178, 291–303. http://dx.doi.org/10.1016/j.agwat.2016.10.009.

Karandish, F., Salari, S., Darzi-Naftchali, A., 2015. Application of virtual water trade to evaluate cropping pattern in arid regions. Water Resour. Manage. 29, 4061–4074. http://dx.doi.org/10.1007/s11269-015-1045-4.

Kirda, C., Cetin, M., Dasgan, Y., Topcu, S., Kaman, H., Ekici, B., Derici, M.R., Ozguven, A.I., 2004. Yield response of greenhouse grown tomato to partial root drying and conventional deficit irrigation. Agric. Water Manage. 69, 191–201.

Kisi, O., Cimen, M., 2009. Evapotranspiration modelling using support vector machines. Hydrol. Sci. J. 54 (5), 918–928.

Klocke, N.L., Schneekloth, J.P., Melvin, S., Clark, R.T., Payero, J.0., 2004. Field scale limited irrigation scenarios for water policy strategies. Appl. Eng. Agric. 20, 623–631.

Lamorski, K., Pastuszka, T., Krzyszczak, J., Stawinski, C., Walczak, B.W., 2013. Soil water dynamic modelling using physical and support vector machine methods. Vadose Zone J. http://dx.doi.org/10.2136/vzj2.13.05.0085.

Lazarovitch, N., Poulton, M., Furman, A., Warrick, A.W., 2009. Water distribution under trickle irrigation predicted using artificial neural networks. J. Eng Math. 64 (2), 207–218. http://dx.doi.org/10.1007/s10665-009-9282-2.

Leonard, R.A., Knisel, W.G., Still, D.A., 1987. GLEAMS: groundwater effects of agricultural management systems. Trans. ASAE 30 (5), 1403–1418.

Lin, G.F., Chen, G.R., Wu, M.C., Chou, Y.C., 2009. Effective forecasting of hourly typhoon rainfall using support vector machines. Water Resour. Res. 45, W08440. http://dx.doi.org/10.1029/2009WR007911.

Liu, D., Yu, Z., Lü, H., 2010. Data assimilation using support vector machines and ensemble Kalman filter for multi-layer soil moisture prediction. Water Sci. Eng. 3, 361–377.

Mguidiche, A., Provenzano, G., Douh, B., Khila, S., Rallo, G., Boujelben, A., 2015. Assessing HYDRUS2D to simulate soil water content (SWC) and salt accumulation under an SDI system: application to a potato crop in a semi-arid area of central Tunisia. Irrig. Drain. 64, 263–274.

Mohandes, M.A., Halawani, T.O., Rehman, S., Hussain, A.A., 2004. Support vector machines for wind speed prediction. Renew. Energy 29, 939–947.

Mualem, Y., 1976. A new model for predicting the hydraulic conductivity of unsaturated porous media. Water Resour. Res. 12, 513–522.

Mubarak, I., 2009. Effect of temporal variability in soil hydraulic properties on simulated water transfer under high-frequency drip irrigation. Agric. Water Manage. 96 (11), 1547–1559.

Neitsch, S.L., Arnold, J.G., Kiniry, J.R., Williams, J.R., 2005. Soil and Water Assessment Tool (SWAT), Theoretical Documentation. Blackland Research Center, Grassland, Soil and Water Research Laboratory, Agricultural Research Service, Temple, TX.

Nishat, S., Guo, Y., Baetz, B.W., 2007. Development of a simplified continuous simulation model for investigating long-term soil moisture fluctuations. Agric. Water Manage. 92, 53–63. http://dx.doi.org/10.1016/j.agwat.2007.04.012.

OECD, 2010. Sustainable Management of Water Resources in Agriculture.

Ozbayoglu, G., Ozbayoglu, M.E., 2006. A new approach for the prediction of ash fusion temperatures: a case study using Turkish lignites. Fuel 85, 545–552.

Ozger, M., Yıldırım, G., 2008. Determining turbulent flow friction coefficient using adaptive neuro-fuzzy computing technique. Adv. Eng. Softw. http://dx.doi.org/10.1016/j.advengsoft.2008.04.006.

Panigrahi, B., Panda, S.N., 2003. Field test of a soil water balance simulation model. Agric. Water Manage. 58, 223–240. http://dx.doi.org/10.1016/S0378-3774(02)00082-3.

Pang, L., Close, M.E., Watt, J.P.C., Vincent, K.W., 2000. Simulation of picloram, atrazine and simazine through two New Zealand soils and into groundwater using HYDRUS2D. J. Contam Hydrol. 44, 19–46.

Parchami-Araghi, F., Mirlatifi, S.M., Ghorbai-Dashtaki, Sh., Mahdian, M.M., 2013. Point estimation of soil water infiltration process using Artificial Neural Networks for some calcareous soils. J. Hydrol. 481 (25), 35–47.

Payero, J.O., Melvin, S.R., Irmak, S., Tarkalson, D., 2006. Yield response of corn to deficit irrigation in a semiarid climate. Agric. Water Manage. 84, 101–112.

Ramos, T.B., Šimůnek, J., Gonçalves, M.C., Martins, J.C., Prazeres, A., Pereira, L.S., 2012. Two-dimensional modeling of water and nitrogen fate from sweet sorghum irrigated with fresh and blended saline waters. Agric. Water Manage. 111, 87–104.

Rehman, S., Mohandes, M., 2008. Artificial neural network estimation of global solar radiation using air temperature and relative humidity. Energy Policy 63 (2), 571–576.

Rahil, M.H., 2007. Simulating soil water flow and nitrogen dynamics in a sunflower field irrigated with reclaimed wastewater. Agric. Water Manage. 92 (3), 142–150.

Ritchie, J.T., 1972. Model for predicting evaporation from a row crop with incomplete cover. Water Resour. Res. 8, 1204–1213.

SAI, Platform Water Working Group, 2010. Principles & Practices for the Sustainable Water Management.

Sayed, T., Tavakolie, A., Razavi, A., 2003. Comparison of adaptive network based fuzzy inference systems and B-spline neuro-fuzzy mode choice models. Water Resour. Res. 17 (2), 123–130.

Sepaskhah, A.R., Ahmadi, S.H., 2010. A review on partial root-zone drying irrigation. Int. J. Plant Prod. 4 (4), 241–258.
Shao, G.C., Zhang, Z.Y., Liu, N., Yu, S.E., Xing, W.G., 2008. Comparative effects of deficit irrigation (DI) and partial rootzone drying (PRD) on soil water distribution, water use, growth and yield in greenhouse grown hot pepper. Sci. Hortic. 119 (1–10), 11–16.
Simon, C., Steven, R., Raine, R., 2009. Physiological response of cotton to a root zone soil moisture gradient: implications for partial root zone drying irrigation. J. Cotton Sci. 13, 67–74.
Šimůnek, J., van Genuchten, M.T., 1996. Estimating unsaturated soil hydraulic properties from tension disc infiltrometer data by numerical inversion. Water Resour. Res. 32 (9), 2683–2696.
Šimůnek, J., van Genuchten, M.Th., Šejna, M., 2008. Development and applications of the HYDRUS and STANMOD software packages and related codes. Vadose Zone J. http://dx.doi.org/10.2136/VZJ2007.0077, 7(2), 587-600.
Šimůnek, J., van Genuchten, M.Th., Šejna, M., 2016. Recent developments and applications of the HYDRUS computer software packages. Vadose Zone J. 15 (7), 25. http://dx.doi.org/10.2136/vzj2016.04.0033.
Siyal, A.A., Skaggs, T.H., 2009. Measured and simulated soil wetting patterns under porous clay pipe sub-surface irrigation. Agric. Water Manage. 96 (6), 893–904.
Skaggs, T.H., Trout, T.J., Šimůnek, J., Shouse, P.J., 2004. Comparison of HYDRUS-2D simulations of drip irrigation with experimental observations. J. Irrig. Drain. Eng. 130, 304–310.
Souza, C.R., Bassoi, L.H., Filho, L.P.M.J., Silva, F.F.S., Viana, L.H., Dantas, B.F., Pereira, M.S., Ribeiro, P.R.A., 2009. Water relations of field-grown grapevines in the Sao Francisci valley, Braizil, under different rootstocks and irrigation strategies. J. Agric. Sci. 66 (4), 436–446.
Stoll, M., Loveys, B., Dry, P., 2000. Improving water use efficiency of irrigated horticultural crops. J. Exp. Bot. 51, 1627–1634.
Stone, L.R., 2003. Crop water use requirements and water use efficiencies. In: Proceedings of the 15th Annual Central Plains Irrigation Conference and Exposition, Colby, Kansas, pp. 127–133.
Tabari, H., Kisi, O., Ezani, A., Hosseinzadeh Talaee, P., 2012. SVM, ANFIS, regression and climate based models for reference evapotranspiration modeling using limited climate data in a semi-arid highland environment. J. Hydrol. 444–445, 78–89.
Tafteh, A., Sepaskhah, A.R., 2012. Application of HYDRUS-1D model for simulating water and nitrate leaching from continuous and alternate furrow irrigated rapeseed and maize fields. Agric. Water Manage. 113, 19–29.
Taiz, L., Zeiger, E., 2006. Plant Physiology. Sinauer Associates, Inc., Publishers, p. 764.
Tang, J.H., Hsiao, H.F., Yeh, W.C., 2010. Forecasting stock market using wavelet transform and neural networks: an integrated system based on artificial bee colony alghoritm. Applied soft computing, Gmodel.
Tang, L.S., Li, Y., Zhang, J., 2005. Physiological and yield responses of cotton under partial root-zone irrigation. Field Crop Res. 94, 214–223.
Vanclooster, M., Viaene, P., Christiaens, K., Ducheyne, S., 1996. WAVE, Release 2.1: Instruction Manual. Institute for Land and Water Management, Katholieke Universiteit Leuven, Vital Decosterstraat 102, B-3000 Leuve, Belgium.
van Dam, J.C., Huygen, J., Wesseling, J.G., Feddes, R.A., Kabat, P., van Walsum, P.E.V., Groenendijk, P., van Diepen, C.A., 1997. Theory of SWAP, version 2.0. Simulation of water flow, solute transport and plant growth in the soilwater-atmosphere-plant environment. Tech. Rep. Dep. Water Resources, DLO Winand Staring Centre, Wageningen, the Netherlands.
van Genuchten, M.T., 1980. A closed-form equation for predicting the hydraulic conductivity of unsaturated soils. Soil Sci. Soc. Am. J. 44, 892–898.
van Genuchten, M.Th., Leij, F.J., Yates, S.R., 1991. The RETC code for quantifying the hydraulic functions of unsaturated soils. EPA Report 600/2-91/065. US Salinity Laboratory, USDA, ARS, Riverside, CA.
Verburg, K., Ross, P.J., Bristow, K.L., 1996. SWIM v2.1 user manual. Div. Rep. 130. CSIRO Division of Soils, Canberra, Australia.
Vapnik, V., 1995. The Nature of Statistical Learning Theory. Springer Verlag, New York, USA.
Vrugt, J.A., Hopmans, J.W., Šimůnek, J., 2001. Calibration of a two-dimensional root water uptake model. Soil Sci. Soc. Am. J. 65 (4), 1027–1037.
Wagenet, R.J., Hutson, J.L., 1987. LEACHM (Leaching Estimation And Chemistry Model) A process-based model of water and solute movement, transformations, plant uptake and chemical reactions in the unsaturated zone. Version 1.0. Dep. of Agronomy, Cornell University, Ithaca, NY.
Wessolek, G., 1989. Einsatz von Wasserhaushalts—Und Photosynthesemodellen in der Ökosystemanalyse. Landschaftsentwicklung und Umweltforschung, Schriftenreihe des FB 14, TU Berlin 61, 164 S.
Xu, H.L., 2009. Application of xerophytophysiology in plant production-partial root drying improves tomato crops. J. Food Agric. Environ. 7 (3–4), 981–988.
Yu, X., Liong, S.Y., 2007. Forecasting of hydrologic time series with ridge regression in feature space. J. Hydrol. 332, 290–302. http://dx.doi.org/10.1016/j.jhydrol.2006.07.003.
Zhou, H., Li, W., Zhang, C., Liu, J., 2009. Ice breakup forecast in the reach of the Yellow River: the support vector machines approach. Hydrol. Earth Syst. Sci. Discuss. 6, 3175–3198.
Zou, P., Yang, J., Fu, J., Liu, G., Li, D., 2010. Artificial neural network and time series models for predicting soil salt and water content. Agric. Water Manage. 97, 2009–2019. http://dx.doi.org/10.1016/j.agwat.2010.02.011.